



The structural differences between patient-derived α -synuclein strains dictate characteristics of Parkinson's disease, multiple system atrophy and dementia with Lewy bodies

Anke Van der Perren¹ · Géraldine Gelders¹ · Alexis Fenyi² · Luc Bousset² · Filipa Brito¹ · Wouter Peelaerts¹ · Chris Van den Haute^{1,3} · Steve Gentleman⁴ · Ronald Melki² · Veerle Baekelandt¹

Received: 16 December 2019 / Revised: 7 April 2020 / Accepted: 7 April 2020 / Published online: 30 April 2020
© The Author(s) 2020

Abstract

Synucleinopathies, such as Parkinson's disease (PD), multiple system atrophy (MSA), and dementia with Lewy bodies (DLB), are defined by the presence of α -synuclein (α SYN) aggregates throughout the nervous system but diverge from one another with regard to their clinical and pathological phenotype. The recent generation of pure fibrillar α SYN polymorphs with noticeable differences in structural and phenotypic traits has led to the hypothesis that different α SYN strains may be in part responsible for the heterogeneous nature of synucleinopathies. To further characterize distinct α SYN strains in the human brain, and establish a structure-pathology relationship, we pursued a detailed comparison of α SYN assemblies derived from well-stratified patients with distinct synucleinopathies. We exploited the capacity of α SYN aggregates found in the brain of patients suffering from PD, MSA or DLB to seed and template monomeric human α SYN in vitro via a protein misfolding cyclic amplification assay. A careful comparison of the properties of total brain homogenates and pure in vitro amplified α SYN fibrillar assemblies upon inoculation in cells and in the rat brain demonstrates that the intrinsic structure of α SYN fibrils dictates synucleinopathies characteristics. We report that MSA strains show several similarities with PD strains, but are significantly more potent in inducing motor deficits, nigrostriatal neurodegeneration, α SYN pathology, spreading, and inflammation, reflecting the aggressive nature of this disease. In contrast, DLB strains display no or only very modest neuropathological features under our experimental conditions. Collectively, our data demonstrate a specific signature for PD, MSA, and DLB-derived strains that differs from previously described recombinant strains, with MSA strains provoking the most aggressive phenotype and more similarities with PD compared to DLB strains.

Keywords Synucleinopathies · α -synuclein · Strains · Neurodegenerative disorders

Introduction

Parkinson's disease (PD), multiple system atrophy (MSA) and dementia with Lewy bodies (DLB) are neurodegenerative disorders which impose a considerable burden on our aging society. These three disorders, grouped together under

Joint first authorship: Anke Van der Perren, Géraldine Gelders, Alexis Fenyi, joint last authorship: Ronald Melki and Veerle Baekelandt.

✉ Anke Van der Perren
Anke.vanderperren@kuleuven.be

✉ Ronald Melki
Ronald.melki@cirs.fr

✉ Veerle Baekelandt
Veerle.baekelandt@kuleuven.be

² Institut François Jacob (MIRCen), CEA, and Laboratory of Neurodegenerative Diseases, CNRS, Fontenay-aux-Roses, France

³ KU Leuven, Leuven Viral Vector Core, Leuven, Belgium

⁴ Neuropathology Unit, Division of Brain Sciences, Department of Medicine, Imperial College London, London, UK

¹ Laboratory for Neurobiology and Gene Therapy, Department of Neurosciences, KU Leuven, Leuven, Belgium

the banner of synucleinopathies, are defined by the presence of α -synuclein (α SYN) aggregates throughout the nervous system but diverge from one another with regard to their clinical and pathological phenotype [19, 20]. PD is typically characterized by a long prodromal phase followed by parkinsonian motor features including bradykinesia, rigidity, and resting tremor [43]. During later stages, dementia affects more than half of all PD patients [1, 24]. The clinical manifestation of DLB is similar to PD but cognitive symptoms emerge typically one year before onset of motor symptoms [32]. Conversely, MSA is mainly characterized by autonomic dysfunction and cerebellar or parkinsonian features [18]. In PD and DLB, α SYN mainly forms large neuronal inclusions called Lewy bodies (LBs) and neurites (LNs) [51, 59], while in MSA, α SYN aggregates are mostly found in the oligodendroglia as glial cytoplasmic inclusions (GCIs) [60]. Aside from being present in an aggregated form in LBs and GCIs, duplications and triplications as well as point mutations in the *SNCA* gene encoding for α SYN have been associated with monogenetic familial forms of PD and DLB [12, 42, 65].

α SYN can adopt different conformations [33, 62], is enriched at the presynaptic terminals and thought to be involved in synaptic transmission and the recycling of synaptic vesicles [7, 55]. Under physiological conditions, α SYN is present as a soluble and natively unfolded monomer [57], probably in equilibrium with α -helical multimeric assemblies [6, 61]. During pathological conditions, α SYN monomers aggregate into high molecular weight β -sheet-rich oligomeric and fibrillar assemblies with each of these assemblies having unique functional and toxic properties [10, 13, 41, 53, 64].

The recently proposed prion-like behavior of α SYN implies that this amyloidogenic protein might act as a pathogenic factor spreading throughout the nervous system [23, 27]. Earlier indications promoting this idea originated from embryonic transplantation studies in PD patients [25, 27]. Along with these observations, direct cell-to-cell transmission of aggregated α SYN was confirmed in multiple experimental systems in cell culture and in vivo using fibrillar recombinant α SYN [15, 21, 23, 28]. The recent generation of pure fibrillar α SYN polymorphs with differences in structural and phenotypic traits has led to the hypothesis that different α SYN strains may be in part responsible for the heterogeneous nature of synucleinopathies [9]. In support of this hypothesis, we have previously shown that inoculation of two distinct recombinant α SYN assemblies, coined “Fibrils” and “Ribbons”, into rat substantia nigra (SN) resulted in remarkable differences in terms of behavior, neuronal integrity, α SYN pathology and spreading [36]. Subsequently, experiments using patient brain homogenates, fractionated or not, have provided more evidence that aggregated human α SYN can

induce neurologic dysfunction when inoculated into the brain of model animals [31, 45, 63]. Indeed, α SYN present in GCI- and LB-enriched brain fractions was found to possess different biological features both in cells and in vivo. The distinct properties of aggregated α SYN were proposed to depend on both seed properties and the intracellular milieu [37]. The limitations of such studies lie within our inability to distinguish what aggregated α SYN per se and additional molecules, ranging from proteins to lipids, which either contaminate those α SYN-rich inclusions or are bound to pathogenic α SYN, trigger upon injection into the central nervous system (CNS) of animal models. To fill this gap and establish a structural-molecular basis for distinct synucleinopathies, we exploited the capacity of pathogenic α SYN aggregates present in the brain of patients suffering from PD, MSA and DLB to seed and template monomeric human α SYN in vitro via a protein misfolding cyclic amplification (PMCA) assay, resulting in pure α SYN fibrillar strains. Recent studies have also reported seeding and templating properties of pathogenic α SYN isolated from the brain or the cerebrospinal fluid of synucleinopathy patients using the same PMCA amplification method or alternatively real-time quaking-induced conversion (RT-QuIC) [11, 47, 52]. However, these studies were mainly focused on in vitro and cellular characterization. To date, a detailed in vivo comparison of pure α SYN assemblies derived from well-stratified patients with PD, MSA and DLB is still lacking.

Although protein aggregation appears to govern synucleinopathy progression, this does not entirely capture the complexity of the disease processes. The role of inflammatory processes within this intricate context, for example, has not been yet disentangled. Extracellular transmission of distinct α SYN strains could impact the immune tolerance and subsequent reaction, affecting neuronal integrity through the release of pro-inflammatory cytokines. As structurally distinct α SYN assemblies expose different polypeptide chains on their surfaces, they trigger helper and cytotoxic T cell responses in patients to different extents [22, 54], substantiating the genome-wide association study (GWAS) link to specific major histocompatibility complex alleles [2].

Here, we compare side-by-side the properties of total human brain homogenates with in vitro amplified α SYN fibrillar assemblies. The capacity of these strains to aggregate in cell culture and to propagate and induce different pathologies and inflammatory responses in vivo upon inoculation in the rat substantia nigra pars compacta (SNpc) was investigated. We demonstrate that despite some heterogeneity between patients, both the homogenates and the PMCA-amplified strains reflect the characteristics of the different synucleinopathies with the MSA strains being the

most aggressive and more similar to the PD-derived strains than to the DLB assemblies.

Materials and methods

Patient collection

Brain tissues from patients suffering from PD, MSA, and DLB as well as age-matched healthy controls were obtained at autopsy from four to six patients per condition through the UK Brain Bank (Imperial College London, UK). The clinicopathological description of the 19 patients is summarized in Table 1. After removal, the brains were hemisected using a mid-sagittal incision. One hemisphere was dissected fresh and the tissue blocks were frozen. The other hemisphere was formalin fixed for diagnostic neuropathological assessment. The extent of α SYN and tau pathology was assessed using Braak staging criteria and Thal amyloid phases were described [3, 4]. Brain regions enriched with α SYN aggregates were identified by histological examination, isolated and processed into brain homogenates. The cingulate cortex was isolated from the brains of the patients with PD and DLB. The cerebellum was obtained from the brains of the patients with MSA. Both regions were also extracted from the healthy control brains.

Brain tissue homogenization

Frozen brain tissues were weighed in falcon tubes (15 or 50 ml depending on the total weight). The samples were diluted five times in PMCA buffer (150 mM KCl, 50 mM Tris-HCl pH 7.5) to obtain a homogenate at 20% (weight:volume). The homogenization was performed by sonication using the SFX 150 Cell Disruptor sonicator with a 3.17 mm microtip probe (Branson) for 1 min, with 10 s pulses followed by 10 s pauses in a biosafety level 3 environment (BSL-3). The homogenates were aliquoted and immediately frozen in liquid nitrogen before storage at -80°C . All contaminated surfaces were cleaned with SDS (1%) [16].

Aggregated α SYN quantification in patients brain homogenates

Aggregated α SYN was quantified using a filter retardation assay and immunoblotting. To this aim, 0.5 mg of brain homogenates were immobilized on cellulose acetate membranes (0.2 μm pore size, Millipore Corp., Bedford, MA) by filtration using a 48-slot slot-blot filtration apparatus

(GE Healthcare). The membranes were blocked in 5% dried skimmed milk and probed with either the 4B12 (Biolegend, cat # 807801) and P-S129 α SYN antibody (mouse 11A5, provided by Elan Pharmaceuticals, Inc., Dublin, Ireland). Following wash with tris buffered saline with triton (TBST), the membranes were incubated with horseradish peroxidase (HRP) conjugated goat-anti-mouse IgG3 secondary antibody (Thermo, cat #M32707) for 1 h at room temperature. Proteins were visualized using ECL reagents (Pierce, USA).

The Cisbio fluorescence resonance energy transfer (FRET) assay (Cisbio, France, cat # 6FASYPEG) was also used to quantify aggregated α SYN in patients' brain homogenates, following the manufacturer's recommendations. Briefly, patient brain homogenates were diluted to 2.5% (W:V) in lysis buffer provided in the HTRF kit. 10 μl of each diluted brain homogenates were loaded into a 96 well plate and mixed with 10 μl of the FRET donor and acceptor antibodies in the kit. The plate was sealed with a film (CmlAB, Danemark, cat#13076-9P-500) and incubated for 20 h at 20°C without shaking in a Thermomixer comfort (Eppendorf, Montesson, France). After incubation, time-resolved FRET was measured upon excitation at 337 nm using a plate reader (CLARIOstar, BMG Labtech, Germany) [14]. The HTRF signal was recorded at two different wavelengths (665 nm and 620 nm). The amount of aggregated α SYN was derived from the 665/620 nm fluorescence ratio and multiplied by 10.000.

Protein misfolding cyclic amplification assay

All operations were performed in BSL-3. Brain homogenates were diluted in PMCA buffer (150 mM KCl, 50 mM Tris-HCl, pH 7.5) containing monomeric α SYN (100 μM) to a final concentration of 2% (W:V), equivalent to 6 mg of brain tissue, as described previously for other tissues [17]. The sample was split in two tubes of PCR strips (BIOplastics, Landgraaf, The Netherlands). PMCA amplification was performed in quadruplicates for each patient using the Q700 generator and a 431MPX horn (Qsonica, Fisher scientific, Illkirch, France). The power of the horn was set to 30% of maximal amplitude. The program of amplification consisted in 15 s of sonication and 5 min pause at 31°C . Every hour, 5 μl were withdrawn from each tube and diluted in 300 μl of 10 μM of Thioflavin T. The amplification was monitored by measuring Thioflavin T fluorescence using a Cary Eclipse Fluorescence Spectrophotometer (Agilent, Les Ulis, France) with fixed excitation and emission wavelength at 440 nm and 480 nm respectively. Cycle 2, 3 and 4 were performed following the same protocol using 1% of the preceding cycle reaction as seeds for PD and DLB cases, 5% for MSA cases. The amounts of brain homogenates and PMCA amplified assemblies used in each amplification reaction were defined

Table 1 Overview of the patients selected for the study

Case	N°	Sex	Age at onset	Duration (years)	Genetics	Cause of death	Clinical diagnosis	Neuropathological diagnosis
PD 1	PD258	M	52	17	PARK2	Not reported	Tremulous parkinsonism with progression to PDD	LBD-Neocortical (α SYN, Braak VI); Tau Braak I, Thal phase 2
PD 2	PD341	M	54	14	/	Parkinson's with dementia	Akinetic-rigid syndrome with progression to PDD, RBD	LBD-Neocortical (α SYN, Braak VI); Tau Braak II, Thal phase 2
PD 3	PD405	M	67	15	/	Not reported	Idiopathic Parkinson's disease with dementia	LBD-Neocortical (α SYN, Braak VI); Tau Braak II, Thal phase ≥ 3
PD 4	PD523	F	68	18	/	Old age	Parkinson's disease	LBD-Neocortical (α SYN, Braak VI); Tau Braak I, Thal phase ≥ 3
MSA1	PD043	M	78	8	/	Not reported	Atypical akinetic-rigid syndrome with prominent ataxia, PSP questioned	MSA; Tau Braak I, Thal phase 2
MSA2	PD080	M	65	6	PARK2	Parkinson's disease	Akinetic-rigid syndrome with autonomic involvement and prominent ataxia. MSA suspected	MSA; Tau Braak I, Thal phase 0
MSA3	PD192	F	52	6	/	Bronchopneumonia	Akinetic-rigid syndrome with prominent bulbar/autonomic involvement: MSA-P, RBD	MSA; Tau Braak I, Thal phase 0
MSA4	PD300	M	68	7	/	Pneumonia, MSA	Tremulous parkinsonism with prominent autonomic involvement: MSA/Parkinson Plus syndrome suspected	MSA; Tau Braak I, Thal phase 0
MSA5	PD333	M	52	8	LRRK2	Respiratory failure, pneumonia	Parkinsonism, MSA questioned	MSA; Tau Braak I, Thal phase ≥ 3
MSA6	PD363	F	61	13	/	Aspiration pneumonia	MSA, bilateral pallidal DBS (with poor response)	MSA; Tau Braak I, Thal phase 1
DLB 1	PD163	M	70	6	/	Cerebrovascular disease, DLB	DLB, RBD	LBD-Limbic; Tau Braak I, Thal phase 2
DLB 2	PD330	F	71	5	/	DLB	DLB	LBD-Neocortical (α SYN, Braak VI); Tau Braak V, Thal phase ≥ 3
DLB 3	PD362	M	84	5	/	Not reported	Progressive cognitive decline (AD?) with abnormal gait	LBD-Neocortical (α SYN, Braak VI); Tau Braak VI, Thal phase ≥ 3
DLB 4	PD385	M	75	5	/	Not reported	DLB, RBD	LBD-Neocortical (α SYN, Braak VI); Tau Braak I, Thal phase ≥ 3
CTR 1	CO28	F	84	n.a	/	Pancreatic cancer	/	No α SYN; Tau Braak II, Thal phase 0
CTR 2	CO29	M	82	n.a	/	Metastatic liver and lung cancer	/	No α SYN; Tau Braak I, Thal phase 1
CTR 3	CO30	M	77	n.a	/	Cardiac failure/ prostate cancer	/	No α SYN; AGD, Thal phase 2
CTR 4	CO34	M	90	n.a	/	Respiratory failure/ bronchial cancer	/	No α SYN; Tau Braak I, Thal phase 0
CTR 5	CO53	F	89	n.a	/	Not reported	Hypertension, Type II diabetes, Hyperthyroidism, Previous CVA	No α SYN; Tau Braak II, Thal phase ≥ 3

The table summarizes the clinical history of the patients included in the study. Information about sex, age at onset, duration of the disease, genetics, cause of death, clinical and neuropathological diagnosis are described

AD Alzheimer's disease, AGD argyrophilic grain disease, α SYN α -synuclein, CVA cerebrovascular accident, DBS deep brain stimulation, DLB dementia with Lewy bodies, F female, LBD Lewy body dementia, LRRK2 leucine-rich repeat kinase 2, M male, MSA multiple system atrophy, MSA-P multiple system atrophy Parkinsonian subtype, n.a. not applicable, PARK2 Parkinson's disease associated gene 2, PDD Parkinson's disease with dementia, PSP progressive supranuclear palsy, RBD rapid eye movement sleep behavior disorder

through an optimization study aimed at maintaining high stringency by minimizing the de novo aggregation of α SYN under our experimental conditions. The time at which an aliquot from one amplification reaction was withdrawn for a subsequent amplification reaction was also defined through an optimization study aimed at avoiding de novo α SYN fibrillar assemblies formation.

At cycle 4, PMCA reactions products were spun for 30 min at 50,000g, the amount of monomeric α SYN in the supernatant was assessed spectrophotometrically and the pelleted assemblies were resuspended in phosphate-buffered saline (PBS) buffer. All resuspended assemblies, at a final concentration of 100 μ M α SYN, were fragmented prior to in vivo use by sonication for 20 min in 2-ml Eppendorf tubes in a Vial Tweeter powered by an ultrasonic processor UIS250v (250 W, 2.4 kHz; Hielscher Ultrasonic, Teltow, Germany), aliquoted, flash frozen in liquid nitrogen and stored until use at -80°C .

Proteolytic digestion

De novo assembled α SYN fibrils and ribbons as well as PD, MSA and DLB patients PMCA-amplified α SYN assemblies (1.4 mg/ml) in 150 mM KCl, 50 mM Tris-HCl, pH 7.5, 1 mM EGTA were treated at 37°C by Proteinase K (3.8 μ g/ml) (Roche). Aliquots were removed at different time intervals following addition of the protease and transferred into Eppendorf tubes maintained at 90°C containing sample buffer (50 mM Tris-HCl, pH 6.8, 4% SDS, 2% beta-mercaptoethanol, 12% glycerol and 0.01% bromophenol blue) to arrest immediately the cleavage reaction. After incubation of each tube for 5 min at 90°C , the samples were processed to monitor the time course of α SYN cleavage by polyacrylamide gel electrophoresis (PAGE) (15%) after staining with Coomassie blue.

Transmission electron microscopy

The morphology of the de novo assembled and PMCA-amplified α SYN assemblies was assessed by transmission electron microscopy (TEM) in a Jeol 1400 transmission electron microscope following adsorption onto carbon-coated 200 mesh grids and negative staining with 1% uranyl acetate. The images were recorded using a Gatan Orius CCD camera (Gatan).

Conformational characterization using FILA4 antibody

α SYN fibrils, ribbons assembled de novo and PMCA-amplified α SYN assemblies (0.2 μ g) in 150 mM KCl, 50 mM Tris-HCl, pH 7.5, were spotted onto single nitrocellulose membranes. The membranes were blocked in 5% dried

skimmed milk and probed with the aggregated α SYN specific antibody FILA4 at a concentration of 0.28 μ g/ml [35]. Following wash with TBST, the membranes were incubated with HRP-conjugated swine-anti-rabbit secondary antibody (DAKO, Copenhagen, Denmark) for 1 h at room temperature. Proteins were visualized using ECL reagents (Pierce, USA). ECL signal was detected using a ChemiDoc™ MP (BioRad) and the protocol “Chemi”. Acquisition was performed using the protocol “Signal Acquisition Mode” from 1 to 60 s of exposure. Images were processed and quantified using Image Lab. The FILA4 signal intensity for each spot was integrated using “Lanes & Bands” function.

α SYN seeding assay

Human H4 neuroglioma cells stably expressing α SYN-YFP fusion protein were seeded at 6000 cells per well in a 384-well plate. Cells were incubated with patient-derived homogenates or PMCA-amplified α SYN assemblies (175 nM). Recombinant α SYN fibrils (175 nM) were used as a positive control. The particle concentration of patient-derived or de novo assembled fibrillar α SYN was obtained by dividing α SYN monomeric concentration by the average number of molecules (as measured by analytical ultracentrifugation (AUC) and TEM). The average number of molecules measured for all amplified α SYN fibrils was 8300 ± 300 . The average length of all amplified fibrils was 41 ± 2 nm. Cells were fixed in 10% paraformaldehyde (PFA) 24 h after incubation with the different brain homogenates or PMCA-amplified α SYN assemblies and were conserved in PBS with DAPI (4',6-diamidino-2-phenylindole, 1/5000) until analysis. The number of α SYN aggregates and P α SYN positive cells was quantified based on YFP or P α SYN fluorescence respectively and the number of cells was determined with DAPI staining using the Operetta High Content Imaging System (PerkinElmer) and Harmony 4.9 software. The width to length ratio and the roundness was determined using the same software. The detailed photographs were taken by a Zeiss LSM 880 confocal microscope.

Primary cortical neuron cultures

Primary cortical neurons were prepared from the cortex of E16 FVB/N mouse embryos. Meninges were removed, cortices were dissected, and subsequently dissociated according to the protocol. Neurons were plated in a 24-well plate with coverslips at a density of 200,000 cells per well. Cells were treated with PMCA-amplified α SYN assemblies (175 nM) in Neurobasal medium supplemented with 2 mM L-glutamine and 2% B27 at DIV 1. Cells were fixed in 10% PFA at DIV 7 for immunocytochemical analysis.

Recombinant AAV production and purification

Vector production and purification was performed as previously described [39]. The plasmids include the constructs for the AAV7 serotype, the AAV transfer plasmid encoding the human mutant A53T α SYN under the control of the ubiquitous CMVie enhanced synapsin1 promoter and the pAdvDeltaF6 adenoviral helper plasmid. Real-time PCR analysis was used for genomic copy determination.

Stereotactic injections

All animal experiments were carried out in accordance with the European Communities Council Directive of November 24, 1986 (86/609/EEC) and approved by the Bioethical Committee of the KU Leuven (ECD project P067-2013 and P085-2014, Belgium). Eight-week-old female Sprague Dawley rats (Janvier, France) weighing about 200 to 250 g were housed under a normal 12-h light and/or dark cycle with free access to pelleted food and tap water. All surgical procedures were performed using aseptic techniques. Rats were anaesthetized with ketamine (60 mg/kg, intraperitoneal (i.p.), Ketalar, Pfizer, Belgium) and medetomidine (0.4 mg/kg, i.p., Dormitor, Pfizer, Belgium). Following anesthesia, the rodents were placed in a stereotactic head frame (Stoelting, IL, USA). Injections were performed with a 30-gauge needle (VWR International, Haasrode, Belgium) and a 10- μ l Hamilton syringe (Hamilton, Bonaduz, GR, Switzerland). Animals were stereotactically injected into the SN with 2.5 μ l of total brain homogenate (20% W:V) or PMCA-product (100 μ M) supplemented with 0.5 μ l of A53T α SYN recombinant adeno-associated viral vector 2/7 (rAAV2/7 vector) ($5.4E + 11$ GC/ml vector dose) or PBS. rAAV control animals were injected with 3 μ l of diluted A53T α SYN rAAV2/7 vector in the SN (equal vector dose). Stereotactic coordinates used for the SN were anteroposterior, $- 5.3$; lateral, $- 2.0$; and dorsoventral, $- 7.2$ calculated from the dura using bregma as reference.

To determine the overall amount of aggregated α SYN using the HTRF Cisbio assay in the brains of animals after inoculation with the different PMCA-amplified α SYN assemblies, 5 μ l of PMCA-product (100 μ M) supplemented with 0.5 μ l of A53T α SYN rAAV2/7 vector ($5.4E + 11$ GC/ml vector dose) were injected over three injection sites in the rat striatum (STR). Stereotactic coordinates used for the STR were anteroposterior, 0.0; lateral, $- 2.0$; and dorsoventral, $- 5.5/- 4.5/- 4.0$ calculated from the dura using bregma as reference. The injection rate was 0.25 μ l/min and the needle was left in place for an additional five minutes before being retracted.

Cylinder test

The cylinder test was used to quantify forelimb use. Contacts made by each forepaw with the wall of a 20-cm-wide clear glass cylinder were scored from the videotapes by an observer blinded to the animal's identity. A total of 25 contacts were recorded for each animal. The number of impaired forelimb contacts was expressed as a percentage of total forelimb contacts. Non-Lesioned control rats should score around 50% in this test.

Immunohistochemical stainings

Rats were sacrificed with an overdose of sodium pentobarbital (200 mg/kg, i.p., Dolethal, Vetoquinol, Belgium) followed by intracardial perfusion with 4% PFA in PBS. After post-fixation overnight in 4% PFA, 50 μ m-thick coronal brain sections were made with a vibrating microtome (HM 650 V, Microm, Germany). IHC was performed on free-floating sections using antibodies against tyrosine hydroxylase (TH, rabbit polyclonal, Ab152, 1:5000, Merck Millipore, Massachusetts, US), phosphorylated α SYN (P-S129 α SYN, mouse 11A5, 1:5000, provided by Elan Pharmaceuticals, Inc., Dublin, Ireland and rabbit, Ab51253, 1:5000, Abcam, Cambridge, UK), Iba1 (goat polyclonal, Ab107159, 1:1000, Abcam), MHC Class II (mouse, MCA46G, 1:250, Serotec), CD4 (mouse, MCA55GA, 1:500, Serotec) and CD8 (mouse, MCA48GA, 1:500, Serotec). Sections were pretreated with 3% hydrogen peroxide for 10 min and incubated overnight with primary antibody in 10% swine, normal goat or rabbit serum (DakoCytomation, Belgium). As secondary antibody (DakoCytomation, Belgium) we used biotinylated anti-rabbit IgG (TH, 1:600), anti-mouse IgG (P-S129 α SYN, 1:600; MHC Class II, CD4 and CD8, 1:300) and anti-goat IgG (Iba1, 1:300), followed by incubation with streptavidin-horseradish peroxidase complex (1:1000, DakoCytomation, Belgium). TH immunoreactivity was visualized using Vector SG (SK-4700, Vector Laboratories, CA) and P-S129 α SYN, Iba1, MHC Class II, CD4 and CD8 immunoreactivity were visualized using 3,3-diaminobenzidine (0.4 mg/ml, Sigma-Aldrich) as a chromogen.

Immunofluorescent stainings

Sections were rinsed three times in PBS and then incubated overnight in PBS-0.1% triton X-100 with 10% donkey serum (Jackson ImmunoResearch Laboratories, Inc., UK) and the following antibodies: mouse anti-P-S129 α SYN (11A5, 1:5000, Elan Pharmaceuticals), chicken anti-TH (THY, 1:1000, Aves) and rabbit anti-GST- π (312, 1:1000, MBL Life Science), mouse anti-P-S129 α SYN (11A5, 1:5000, Elan Pharmaceuticals), rabbit anti-Olig2 (Ab9610, 1:1000,

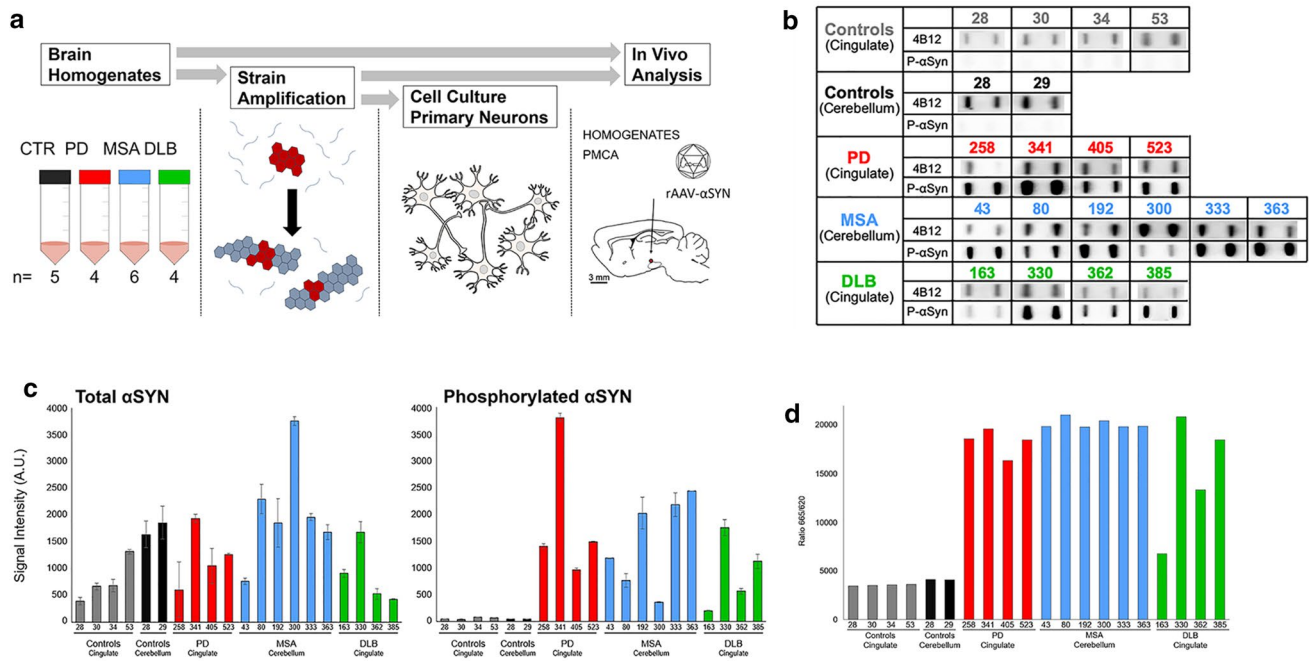


Fig. 1 Quantification of aggregated α SYN in patients' brains. **a** Schematic representation of the experimental setup. Brain tissues from patients suffering from PD, MSA and DLB as well as age-matched healthy controls ($n=4-6$) were obtained at autopsy and processed into total brain homogenates. The pathogenic α SYN aggregates present in the patient's brain were utilized to seed and template monomeric human α SYN in vitro via a PMCA assay. Total brain homogenates and in vitro amplified α SYN fibrillar assemblies were carefully compared upon administration to cell culture and upon inoculation in the rat brain. **b** The amount of pathogenic, aggregated α SYN in the

different brain homogenates was determined using a filter retardation assay. 50 μ l of brain homogenates (1% in PBS, W:V), equivalent to 0.5 mg total proteins, were filtered on cellulose acetate membranes and probed with 4B12 (total α SYN) or anti-phosphorylated α SYN (P α SYN). **c** Quantification of total α SYN and P α SYN in the different brain homogenates presented in panel b. **d** The amount of pathogenic, aggregated α SYN in the different brain homogenates (2.5% in PBS, weight:volume) was quantified using the Cisbio FRET assay as described in the "Materials and methods" section

Merck Millipore) or mouse anti-DARPP-32 (H3, Santa Cruz Biotechnology 1:500). After three rinses in PBS-0.1% triton X-100 the sections were incubated in the dark for 2 h in fluorochrome-conjugated secondary antibodies: donkey anti-mouse Alexa 488 (1:1000, Molecular Probes™, Invitrogen, Belgium), donkey anti-chicken Cy3 (1:500, Jackson ImmunoResearch) and donkey anti-rabbit Alexa 647 (1:1000, Molecular Probes™, Invitrogen) or donkey anti-mouse Alexa 488 (1:1000, Molecular Probes™, Invitrogen, Belgium) and donkey anti-rabbit Alexa 647 (1:1000, Molecular Probes™, Invitrogen). After being rinsed in PBS and mounted, the sections were coverslipped with Mowiol 4-88 (Calbiochem®, California, US) and DAPI (1:1000).

For immunocytochemical analysis, fixed coverslips were incubated overnight in PBS-0.1% triton X-100 with 10% donkey serum (Jackson ImmunoResearch Laboratories, Inc., UK) and primary antibodies against mouse P-S129 α SYN (11A5, 1:5000, Elan Pharmaceuticals) and rabbit β 3-tubulin (Ab52901, 1:1000, Abcam). The secondary antibodies used were donkey anti-mouse Alexa 488 (1:1000, Molecular Probes™, Invitrogen, Belgium) and donkey anti-rabbit Alexa 647 (1:1000, Molecular Probes™, Invitrogen,

Belgium). Fluorescent stainings were visualized by confocal microscopy with an LSM 880 unit (Zeiss, Belgium).

Stereological quantification

The number of TH- and P-S129 α SYN positive cells in the SN was determined by stereological measurements using the Optical fractionator method in a computerized system as described before [5] (StereoInvestigator; MicroBright-Field, Magdeburg, Germany). Every fifth section throughout the entire SN was analyzed, with a total of seven sections for each animal. The coefficients of error, calculated according to the procedure of Schmitz and Hof as estimates of precision [46], varied between 0.05 and 0.10. All the analyses were performed by an investigator blind to different groups.

Striatal immunoreactivity quantification

Seven sections covering the whole STR were stained using an antibody against TH as previously described. Images were acquired using the LEICA DM6B optical microscope

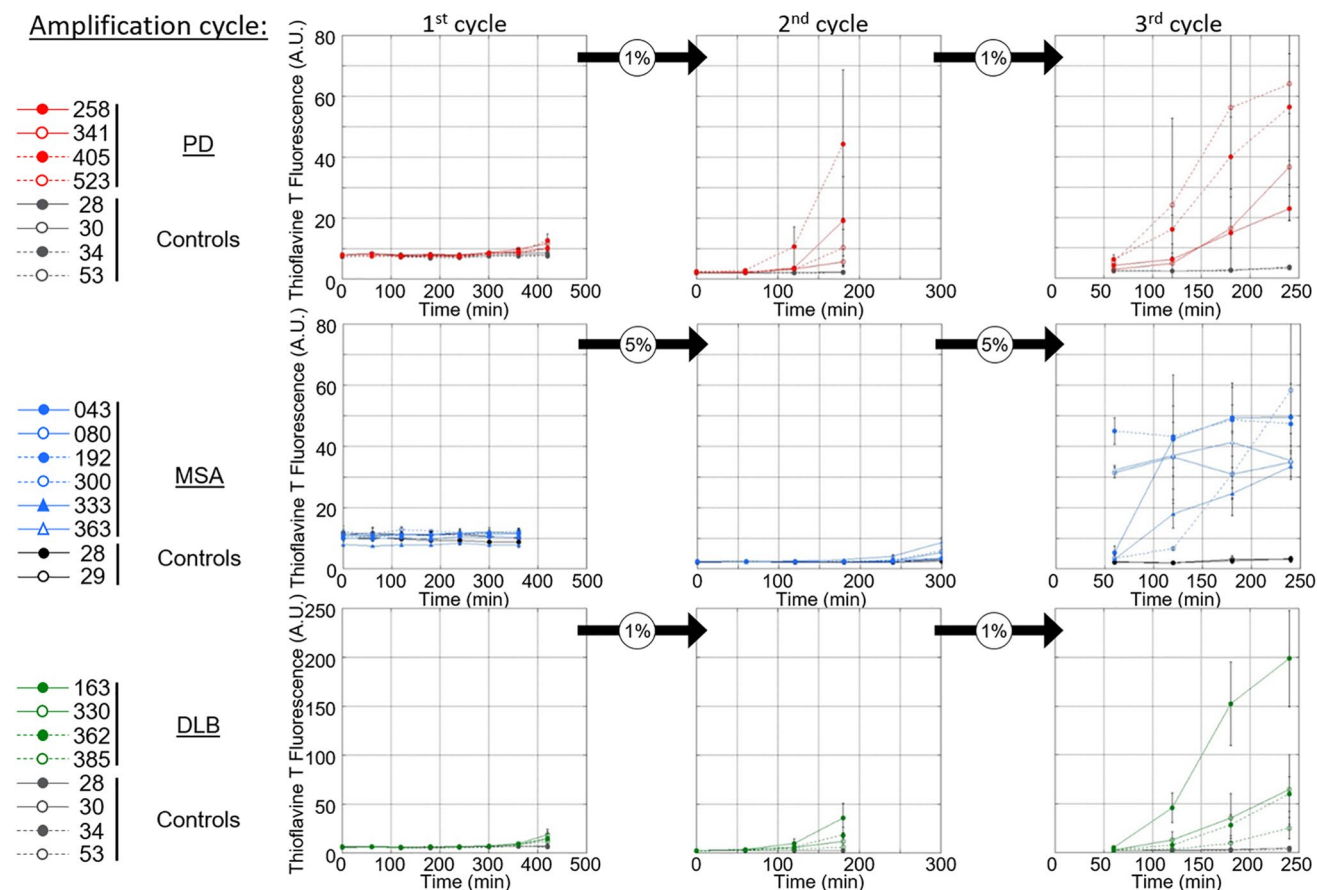


Fig. 2 Amplification of pathogenic α SYN from PD, MSA and DLB patients by PMCA. PMCA was performed on human brain homogenates (2% (W:V) for the 1st cycle, the indicated amounts (V:V) for the next cycles, in PMCA buffer containing monomeric α SYN, 100 μ M) from PD (top, in red), MSA (middle, in blue), DLB (bottom, in green) and the corresponding control (in black or gray) patients. The amounts of brain homogenates and PMCA-amplified assemblies used in each amplification reaction were defined through an optimiza-

tion study aimed at maintaining high stringency by minimizing the de novo aggregation of α SYN under our experimental conditions. The time at which an aliquot from one amplification reaction was withdrawn for a subsequent amplification reaction was also defined through an optimization study aimed at avoiding the formation of de novo of α SYN fibrillar assemblies. The curves represent an average of four replicates \pm SD

(Leica, Wetzlar, Germany) with a Leica DFC 7000 T digital camera (Leica) and the Leica Application Suite software (Leica). Intensity measurement was performed using the software ImageJ.

Evaluation of the spreading of α SYN pathology

Spreading of the α SYN pathology was analyzed and scored by immunohistochemical analysis using an antibody against P-S129 α SYN as previously described. Data are shown as heat maps to illustrate the distribution of the α SYN pathology throughout seven different brain regions in a semi-quantitative manner. The selected brain regions are the following: (1) and (2) adjacent sections of caudate putamen (CPu) (respectively bregma 2.16; bregma 1.20); (3) lateral caudate putamen (CPu) and internal capsule

(ic) (bregma – 1.80); (4) SNpc and cerebral peduncle (cp) (bregma – 4.36); (5) dorsal tier of substantia nigra pars compacta (SNpc) and pars reticulata (SNpr) (bregma – 5.28, injection site); (6) medial and ventral tier of SNpc (bregma – 5.76) and (7) lateral SNpc and SNpr (bregma – 6.24).

Results

In vitro characterization of patient-derived α SYN strains

To investigate the presence of distinct human α SYN strains in vivo we analyzed brain specimens from four to six deceased patients carrying the clinical and neuropathological diagnosis of PD, DLB or MSA, as well as five age-matched control patients (CTR). The clinicopathological

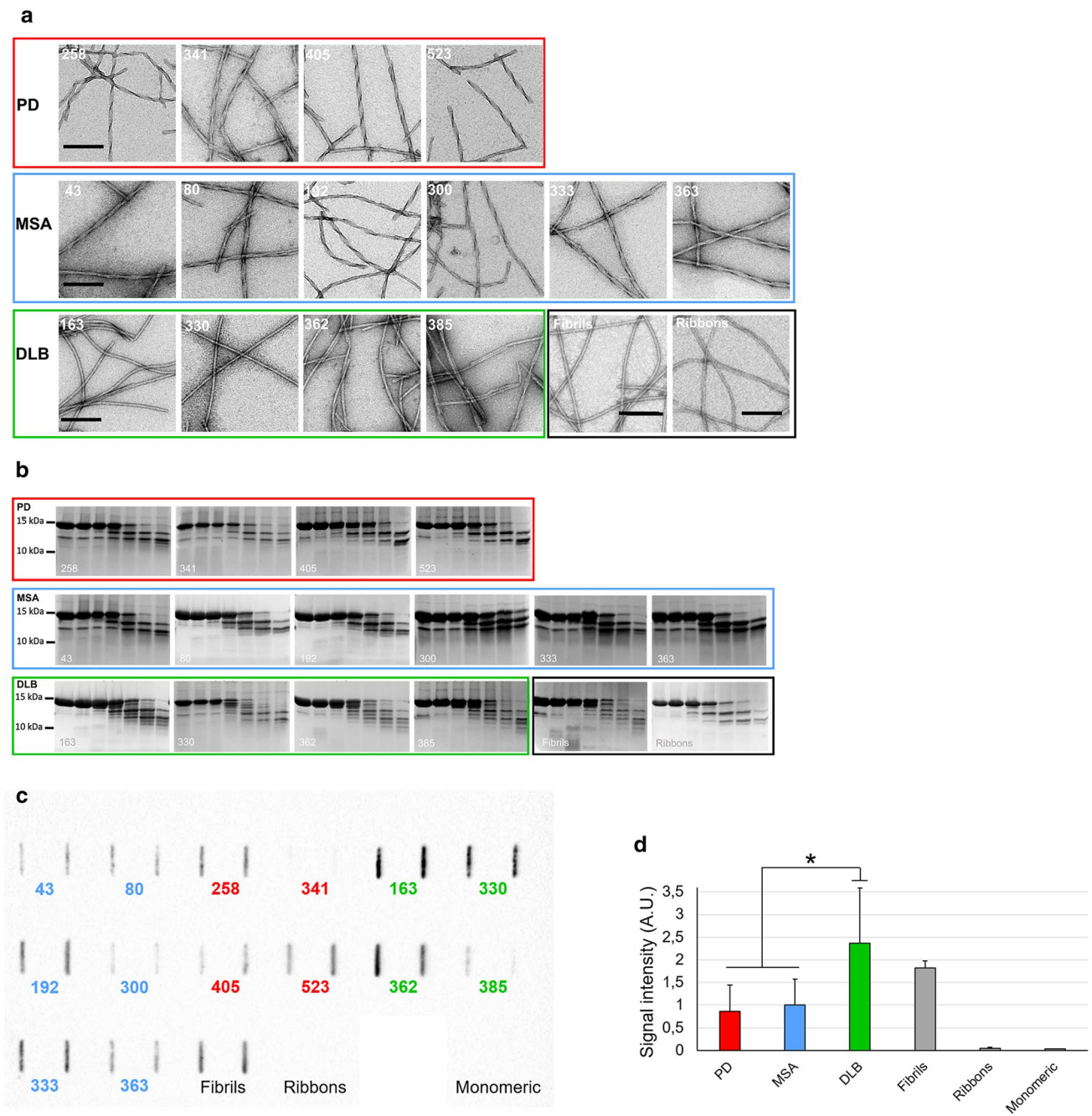


Fig. 3 In vitro characterization of patient-derived α SYN assemblies. **a** Electron micrographs of α SYN assemblies obtained after the 3rd cycle of amplification by PMCA from PD, MSA and DLB patients and from de novo generated α SYN Fibrils and Ribbons. Scale bar=200 nm. **b** Limited proteolytic patterns of α SYN assemblies obtained after the 3rd cycle of amplification by PMCA from PD, MSA and DLB patients and from de novo generated α SYN Fibrils and Ribbons. Monomeric α SYN concentration is 100 μ M. Proteinase K concentration is 3.8 μ g/ml. Samples were withdrawn from the reaction before PK addition (lane most to the left), immediately after PK addition (second lane from left) and at time 1,

5, 15, 30 and 60 min from left to right in all panels. PAGE analysis was performed as described in the “Materials and methods” section and the gels were stained with Coomassie blue. The molecular weight markers are shown on the left. **c** The conformational FILA4 antibody distinguishes equal amounts (0.2 μ g) of PMCA-amplified α SYN strains spotted on a single nitrocellulose membrane. **d** Quantification of FILA4 signal for PD, MSA, DLB, and reference samples (Fibrils, Ribbons, and monomeric α SYN). Data represent mean \pm SE (* p < 0.05 for one-way ANOVA, n = 4–6 PD- or MSA-amplified strains versus DLB-amplified strain)

description of the 19 patients is summarized in Table 1. LB-rich regions were selected, e.g. the cingulate cortex for PD and DLB and the cerebellum for MSA patients, which were subsequently processed into crude homogenates (Fig. 1a). The amount of aggregated α SYN and α SYN phosphorylated at Ser129 (P α SYN) was assessed by filter trapping (Fig. 1b). The amount of α SYN and P α SYN trapped on the cellulose acetate membranes varied significantly amongst PD, MSA or DLB patients (Fig. 1b, c), but was significantly higher in PD, DLB or MSA than in control patient brain homogenates. Very low levels, if any, of aggregated P α SYN was detected in control patients (Fig. 1b, c). The amount of aggregated α SYN was also quantified using the HTRF Cis-bio assay [14]. Similar to what was observed using the filter trap assay, the amounts of aggregated α SYN in PD, DLB or MSA patient brain homogenates were significantly higher than those in control patients (Fig. 1d).

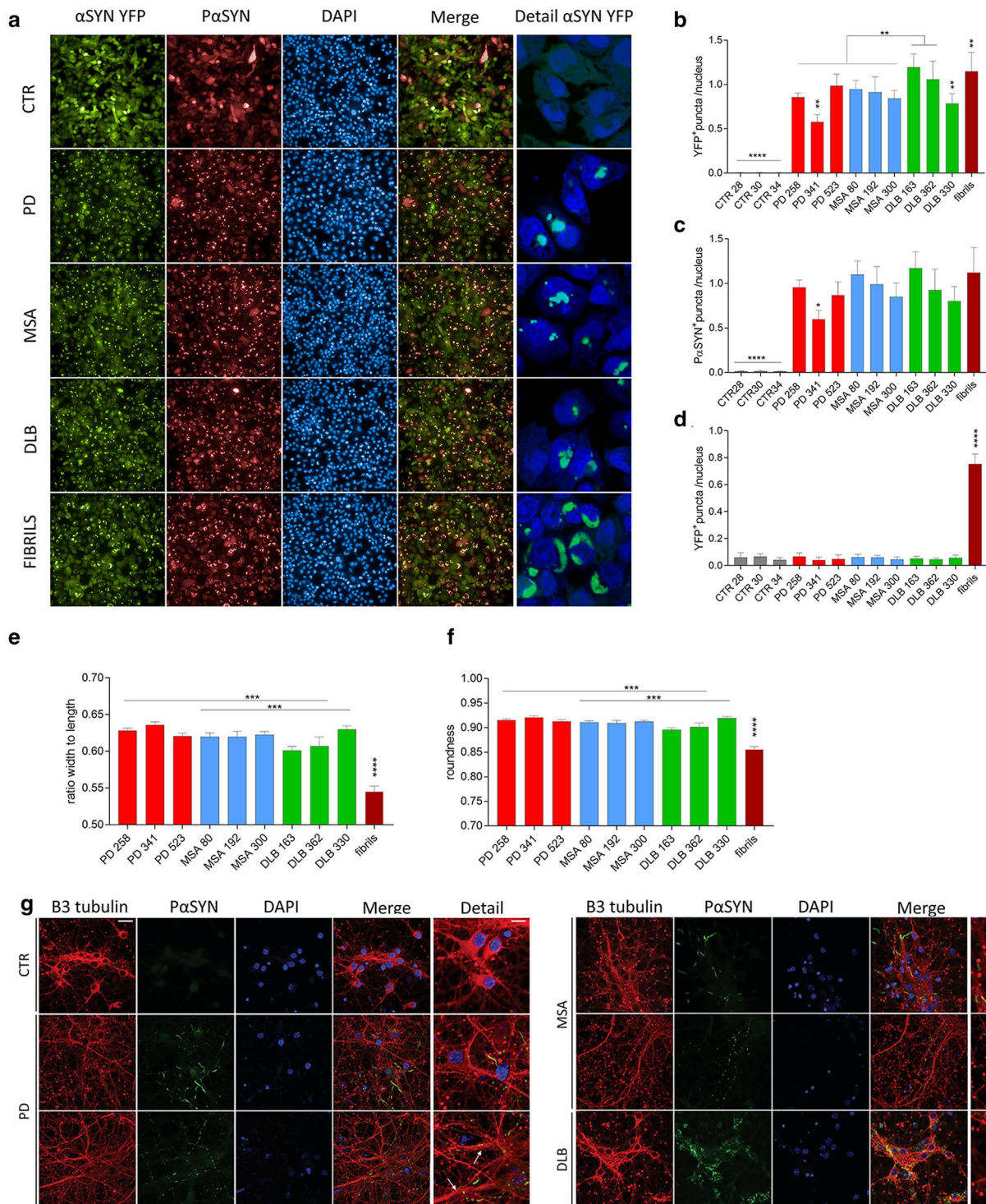
We next used a PMCA assay we implemented to template monomeric α SYN assemblies into pathogenic aggregates that reproduce the structural characteristics of aggregated α SYN in patient brains [17]. Amplification was performed in an iterative manner to ensure that monomeric α SYN does not assemble into fibrils de novo under our experimental conditions. The seeded assembly of monomeric α SYN (100 μ M) in the presence of diseased brain homogenates (2% in assembly buffer) was monitored using Thioflavin T binding (Fig. 2, left panels). After 6 h, the aggregation solution was diluted (20-fold for MSA patients, 100-fold for PD and DLB patients) in assembly buffer containing 100 μ M monomeric α SYN under which the aggregation reaction was further monitored (Fig. 2, central panels). A third round of templating was initiated by diluting the fibrillar assemblies generated (after 5 h for MSA patients, and 3 h for PD and DLB patients) in assembly buffer containing monomeric α SYN (Fig. 2, right panels). Control brain homogenates did not exhibit any seeding potential under the stringent experimental conditions (Fig. 2). The α SYN fibrillar assemblies were imaged by TEM and their limited proteolytic patterns upon exposure to Proteinase K were analyzed by SDS-PAGE. TEM analysis revealed disease-specific differences in the shape of the fibrils. PD and MSA patient-derived α SYN fibrils obtained by PMCA exhibited a relatively flat and twisted appearance, significantly resembling the fibrillar polymorph “Ribbons” (Fig. 3a). Those derived from DLB patients were cylindrical, exhibiting no twists and indistinguishable from the fibrillar polymorph “Fibrils” (Fig. 3a). Furthermore, PMCA-derived PD and MSA α SYN fibrils exhibited similar limited proteinase K degradation patterns that differed from those derived from DLB patients (Fig. 3b). Limited proteolysis patterns of PD and MSA patient-derived α SYN fibrils resembled that of the fibrillar polymorph “Ribbons” while the proteolysis pattern of DLB patient-derived α SYN fibrils was similar to the fibrillar polymorph “Fibrils”

Fig. 4 Characterization of patient-derived α SYN strains in cellular models. **a** Representative photomicrographs of the human neuroglioma (H4) cells stably expressing α SYN-YFP upon administration of the different PMCA-amplified α SYN strains (175 nM; green) or recombinant α SYN fibrils (175 nM; green) stained for P α SYN (red). DAPI was used to visualize the nuclei (blue) (left panel). Detailed photomicrographs of the YFP⁺ puncta present in the H4 cells upon administration of the different PMCA-amplified α SYN strains (right panel). **b** The number of YFP⁺ puncta per nucleus in H4 cells (presented in panel a) was quantified 24 h after incubation with the different PMCA-amplified α SYN strains. **c** The number of P α SYN⁺ puncta per nucleus in H4 cells (presented in panel a) was quantified 24 h after incubation with the different PMCA-amplified α SYN strains. **d** The number of YFP⁺ puncta per nucleus in H4 cells was quantified 24 h after incubation with total brain homogenates. **e** The width to length ratio in H4 cells was measured 24 h after incubation with the different PMCA-amplified α SYN strains. **f** The roundness in H4 cells was measured 24 h after incubation with the different PMCA-amplified α SYN strains. Results shown as mean \pm SEM (** p < 0.01, *** p < 0.001, **** p < 0.0001 for one-way ANOVA with Tukey’s post-hoc analysis, n = 3 patients per condition). **g** Representative photomicrographs of the primary cortical neurons after incubation with the different PMCA-amplified α SYN strains for 7 days stained for the neuronal marker β 3-tubulin (red) and for P α SYN (green). DAPI was used to visualize the nuclei (blue). This experiment was repeated three times. Scale bar represents 10 μ m

(Fig. 3b). Last, we further characterized the PMCA-amplified α SYN assemblies using the conformational antibody FILA4. All PMCA-amplified patient-derived α SYN fibrils were recognized by the aggregated α SYN conformational antibody FILA4 to a different extent (Fig. 3c). In line with our results generated by TEM and limited Proteinase K degradation, PMCA-derived PD and MSA α SYN fibrils were conformationally distinguishable from patient-derived DLB fibrils as significantly lower FILA4 signal was detected in those samples (Fig. 3d). We conclude from these observations that fibrils derived from patients developing one given synucleinopathy have comparable fingerprints and morphology. We further conclude that PD and MSA patient-derived fibrils have a similar shape and limited proteolysis pattern, distinct from that of DLB patient-derived fibrils.

PD, MSA and DLB patient-derived fibrillar α SYN assemblies induce the aggregation of endogenous α SYN in cell culture

We next assessed the seeding capacity of the distinct PMCA-amplified α SYN fibrillar strains in a human H4 neuroglioma cell line expressing α SYN-YFP. Patient-derived or de novo assembled fibrillar α SYN were fragmented to generate fibrillar particles with an average size of 42–52 nm that are suitable for endocytosis, as described in the “Materials and methods” section. There was no difference in the average size of aggregates for the different diseases. The particle concentration of patient-derived or de novo assembled fibrillar α SYN was assessed by AUC and was quantitatively analyzed



by TEM as previously described [41, 48, 49]. Recombinant α SYN fibrils were used as a positive control. Exposure of H4 cells to all α SYN strains for 24 h led to α SYN aggregation as quantified by the number of YFP⁺ puncta per H4 cell nucleus (Fig. 4a, b). No such aggregation was observed upon exposure of H4 cells to CTR samples (Fig. 4a, b) or brain homogenates (Fig. 4d). Aggregated α SYN-YFP co-localized

to a large extent with P α SYN aggregates (Fig. 4c). Recombinant fibrils induced the highest number of YFP⁺ puncta and gave rise to large crescent-shaped YFP⁺ P α SYN⁺ aggregates in H4 cells (Fig. 4a, b). When the patients were grouped per disease, the DLB group showed most inclusions, followed by the MSA patients and then the PD group (Fig. 4b). Analysis per patient revealed that the number of YFP⁺ puncta was

significantly higher in α SYN strains derived from two DLB patients (DLB163 and DLB 362) compared to all the other experimental conditions (PD, MSA and DLB 330). Human H4 cells incubated with α SYN strains from PD 341 exhibited less YFP⁺ aggregates in contrast to the two other PD patients (PD 258 and 523). Next, we assessed the morphology of the aggregates. H4 cells incubated with recombinant α SYN fibrils presented inclusions with a significantly reduced width to length ratio and roundness compared to the patient-derived material. In addition, the inclusions from the DLB group displayed a slightly reduced width to length ratio and roundness when compared to the PD and MSA conditions (Fig. 4e, f). Taken together, these data demonstrate that the distinct PMCA-amplified α SYN strains seed monomeric α SYN aggregation in cell culture towards a different extent. Exposure of primary cortical neurons for 7 days to the different PMCA-amplified α SYN fibrillar strains, but not control samples, led to the formation of phosphorylated α SYN deposits (Fig. 4g). Interestingly, we observed a distinct phosphorylation pattern for the different PMCA-amplified α SYN fibrillar strains. Neurons exposed to MSA and PD patient-derived α SYN strains presented two morphologically distinct types of P α SYN-positive neurites, namely thicker linear neurites (top panel) and neurites containing a dotted phosphorylation pattern (lower panel). Those incubated with α SYN strains derived from DLB patients, however, displayed diffuse P α SYN deposits within the soma, surrounding the nucleus. In addition, we also observed differences in β 3 tubulin staining among the experimental conditions. Neurons treated with PD and MSA α SYN strains presented larger dystrophic neurites compared to the CTR or DLB α SYN strains, indicative of ongoing neurodegeneration (Fig. 4g detail). These findings further suggest that distinct PMCA-amplified α SYN strains seed the aggregation of endogenous α SYN to different extents and induce different phenotypic changes.

Intracerebral inoculation of PD, MSA and DLB patient-derived α SYN strains trigger changes in motor behavior

To determine whether the distinct characteristics of α SYN strains reflect in vivo, we inoculated brain homogenates from PD, MSA and DLB patients in parallel with pure PMCA-amplified α SYN assemblies derived from those patients into the rat SN in absence or presence of a rAAV2/7 vector encoding human α SYN (Fig. 5a). A total of 12–16 animals per group was included in this study, representing 4–6 patients per condition and 3 animals per patient. We have previously demonstrated that rAAV-mediated expression of α SYN in the rodent brain induces time-dependent neuropathological changes reminiscent of Lewy pathology [40]. In addition, a more robust

model was generated by the combination of rAAV- α SYN injection into the brain with recombinant protein, resulting in enhanced neurodegeneration and motor behavior, as well as more pronounced Lewy body-like inclusions and protein spreading [36]. To monitor behavioral performance, we subjected the animals to the cylinder test on a monthly basis for five months (Fig. 5b). Neither the brain homogenates nor the PMCA-amplified assemblies induced significant motor deficits in naive animals within the experimental time frame (Fig. 5c, e). When we combined patient-derived material with rAAV-mediated α SYN expression, clear motor deficits developed progressively over time from 3 months post injection and onwards. The MSA patient brain homogenates induced the most prominent motor deficits compared to the CTR patients (MSA, $11 \pm 4\%$ remaining forepaw use versus CTR, $36 \pm 7\%$, Fig. 5d). Animals injected with rAAV- α SYN alone or together with PMCA-amplified α SYN assemblies derived from CTR, PD or MSA patients presented similar motor deficits (Fig. 5f). Surprisingly the animals injected with PMCA-amplified α SYN assemblies derived from DLB patients did not display detectable motor deficits. To rule out any technical issues we inoculated an additional group of animals with PMCA-amplified α SYN assemblies derived from DLB and MSA patients ($n = 8$ –12 animals per condition) and similar results were obtained (data not shown). We conclude from these findings that rats robustly develop motor deficits only when brain homogenates from PD, MSA and DLB patients, and to a much lesser extent PMCA-amplified α SYN assemblies derived from those cases, are delivered into their SN in the presence of additional soluble human α SYN supplied by a rAAV- α SYN expression vector.

PD, MSA and DLB patient-derived α SYN strains exhibit distinct dopaminergic neurotoxicity

Nigral inoculation of brain homogenates in naive rats led to a decrease in the number of tyrosine hydroxylase (TH) positive neurons with the MSA and DLB groups having the highest proportion of neuronal loss ($41 \pm 5\%$ and $49 \pm 8\%$ respectively) compared to the PD and CTR groups ($27 \pm 7\%$ and $28 \pm 4\%$ respectively) at the final time point of 150 days (Fig. 6a). rAAV-mediated expression of human α SYN resulted in $25 \pm 5\%$ nigral dopaminergic cell loss. Upon co-injection with brain homogenates, additional cell loss was observed for the MSA and PD groups ($74 \pm 3\%$ and $61 \pm 6\%$ respectively) but not for the DLB and CTR groups ($44 \pm 6\%$ and $30 \pm 12\%$; Fig. 6b, c). Nigral inoculation of PMCA-amplified α SYN assemblies in naive rats only induced mild dopaminergic cell loss (ranging from 21–28%) with no differences between

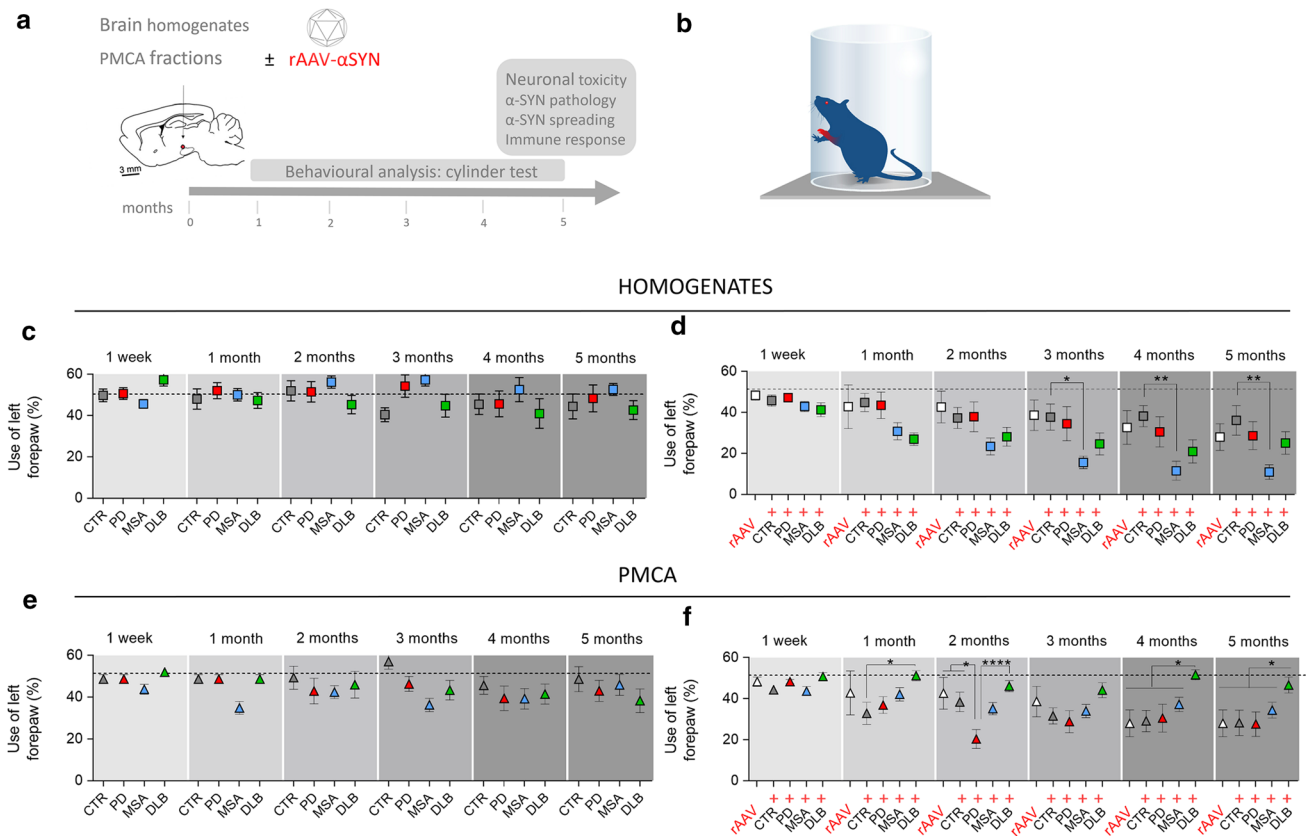


Fig. 5 Assessment of motor deficits after intracerebral inoculation of the different patient-derived homogenates and PMCA-amplified αSYN strains. **a** Schematic representation of the experimental set-up. Rats were inoculated with the different patient-derived brain homogenates or PMCA-amplified αSYN strains in absence or presence of human αSYN expression. Animals were subjected to the cylinder test on a monthly basis. The in vivo behavior of the distinct human αSYN strains was characterized by assessing neuronal toxicity, αSYN pathology, spreading of αSYN pathology and inflammatory response at the final time point of 150 days. **b** Schematic drawing illustrating the set-up of the cylinder test to assess motor behavior. **c, d** Altera-

tions in motor behavior after inoculation of PD, MSA, DLB patient-derived homogenates and age-matched controls in absence (**c**) or presence of rAAV2/7-mediated overexpression of αSYN (rAAV) (**d**) were assessed using the cylinder test. **e, f** Alterations in motor behavior after inoculation of PD, MSA or DLB-derived PMCA-amplified αSYN assemblies in absence (**e**) or presence of rAAV-αSYN overexpression (**f**) were assessed using the cylinder test. Results shown as mean ± SEM (* $p < 0.05$, ** $p < 0.01$, **** $p < 0.0001$ for two-way ANOVA with Tukey's post-hoc analysis, $n = 4-6$ patients per group and $n = 3$ per patient). A total of 12–16 animals per group was included in this study

the different experimental groups (Fig. 6d). In line with the results obtained with brain homogenates, combining rAAV-αSYN expression with PMCA-amplified MSA and PD assemblies had an additive effect ($62 \pm 4\%$ and $53 \pm 6\%$ respectively) unlike PMCA-amplified DLB and CTR assemblies ($26 \pm 5\%$ and $14 \pm 3\%$; Fig. 6e, f). Quantifications of striatal dopaminergic nerve terminals further revealed that inoculation of both the brain homogenates or the PMCA-amplified αSYN assemblies in naive rats did not induce a significant striatal lesion at the final time point of 150 days (Fig. 6g, i). However, upon inoculation of brain homogenates in the presence of rAAV-αSYN, significant striatal lesions were induced for all diseases with the most prominent loss for MSA patient brain homogenates ($60 \pm 8\%$, Fig. 6h). Similarly, prominent striatal lesions were observed in animals co-injected with

rAAV-αSYN and PMCA-amplified assemblies from PD and MSA patients but not from DLB patients (Fig. 6j).

PD, MSA and DLB patient-derived αSYN strains induce distinct αSYN pathology and spreading

To assess αSYN pathology, we first analyzed the number of PαSYN positive nigral neurons. Injection of PD, MSA and DLB patient brain homogenates or PMCA-amplified assemblies in naive rats resulted in a low number of PαSYN positive dopaminergic neurons (Fig. 7a, left). In contrast, combining rAAV-driven αSYN expression with PD, MSA and DLB patient brain homogenates or PMCA-amplified assemblies led to overall increased numbers of PαSYN positive cells (Fig. 7a, right). Interestingly, the number of nigral PαSYN positive cells was significantly higher in animals

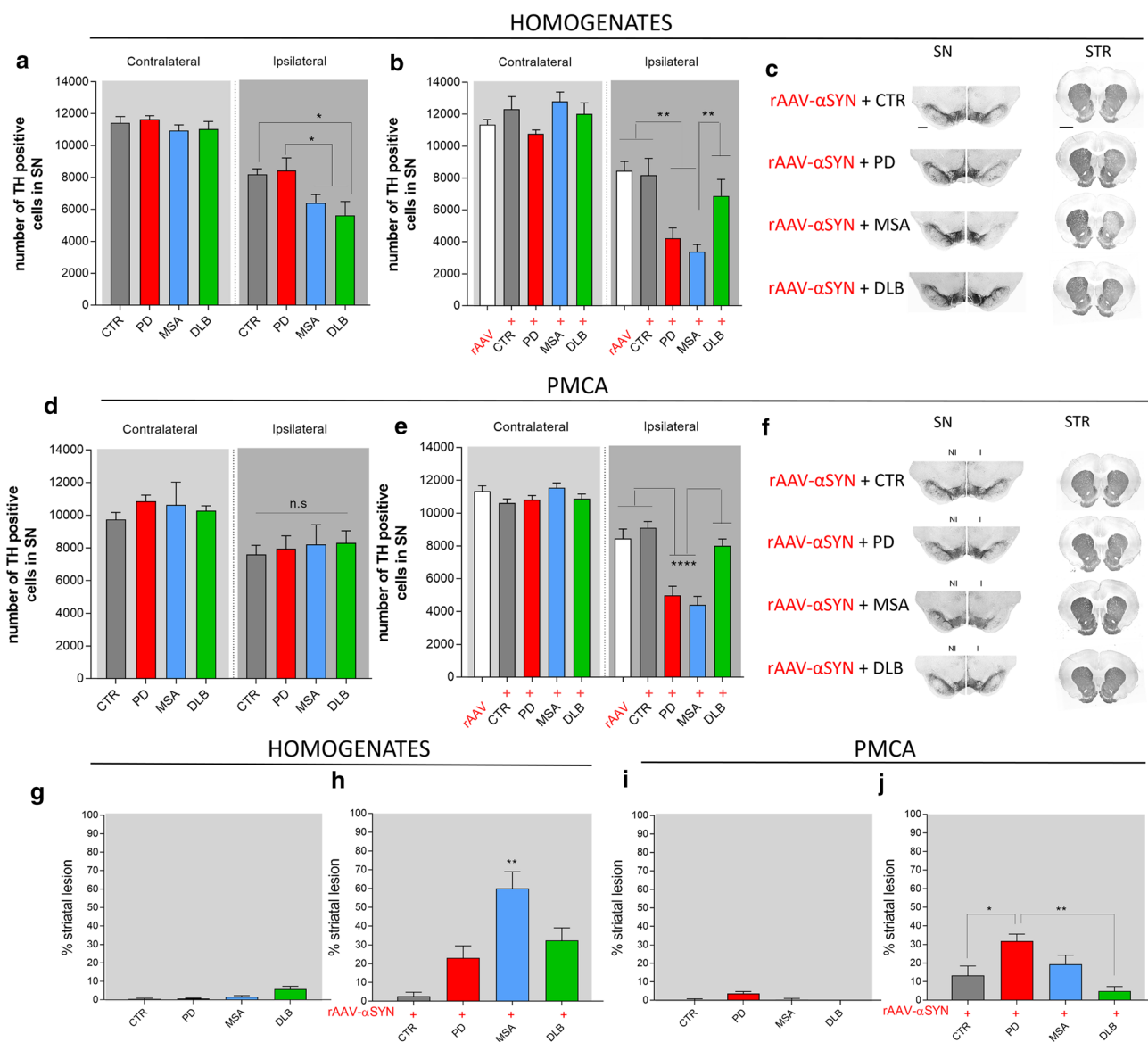


Fig. 6 Dopaminergic neurodegeneration after intracerebral inoculation of different patient-derived homogenates and PMCA-amplified α SYN strains. **a, b** Stereological quantification of the number of TH⁺ cells in the rat SN 5 months after inoculation of patient-derived homogenates in absence (**a**) or presence (**b**) of rAAV2/7- α SYN overexpression (rAAV). **c** Representative images of TH staining in the SN and striatum five months after co-injection of the patient-derived homogenates and human α SYN overexpression. Scale bar represents 400 μ m (SN) and 1000 μ m (STR). **d, e** Stereological quantification of the number of TH⁺ cells in the rat SN five months after inoculation of PMCA-amplified α SYN in absence (**d**) or presence (**e**) of rAAV2/7- α SYN overexpression. **f** Representative images of TH staining in the SN and striatum five months after co-injection of PMCA-amplified α SYN assemblies and human α SYN expression. Results shown as

mean \pm SEM (* p < 0.05, ** p < 0.01, **** p < 0.0001 for two-way ANOVA with Bonferroni post-hoc analysis, n = 4–6 patients per group and n = 3 per patient). A total of 12–16 animals per group was included in this study. **g, h** TH striatal lesion was assessed 5 months after inoculation of patient-derived homogenates in absence (**g**) or presence (**h**) of rAAV2/7- α SYN overexpression. **(i, j)** TH striatal lesion was assessed five months after inoculation of PMCA-amplified α SYN assemblies in absence (**i**) or presence (**j**) of rAAV2/7- α SYN overexpression. Results shown as mean \pm SEM (* p < 0.05, ** p < 0.01, **** p < 0.0001 for one-way ANOVA with Tukey's post-hoc analysis, n = 4–6 patients per group and n = 3 per patient). A total of 12–16 animals per group was included in this study. *I* injected, *NI* non-injected, *n.s.* not significant, *SN* substantia nigra, *STR* striatum

of the MSA group when compared to the PD, DLB or CTR groups (Figs. 7b, 8a). This marked P α SYN pathology is in line with the observed severe motor deficits and prominent nigral cell loss (Figs. 5d and 6b). Intriguingly, a significantly

lower number of P α SYN positive cells was observed when rAAV- α SYN was co-injected with PMCA-amplified DLB assemblies (Fig. 7c). DLB brain-derived PMCA assemblies appeared to reduce the number of P α SYN cells (Figs. 7c,

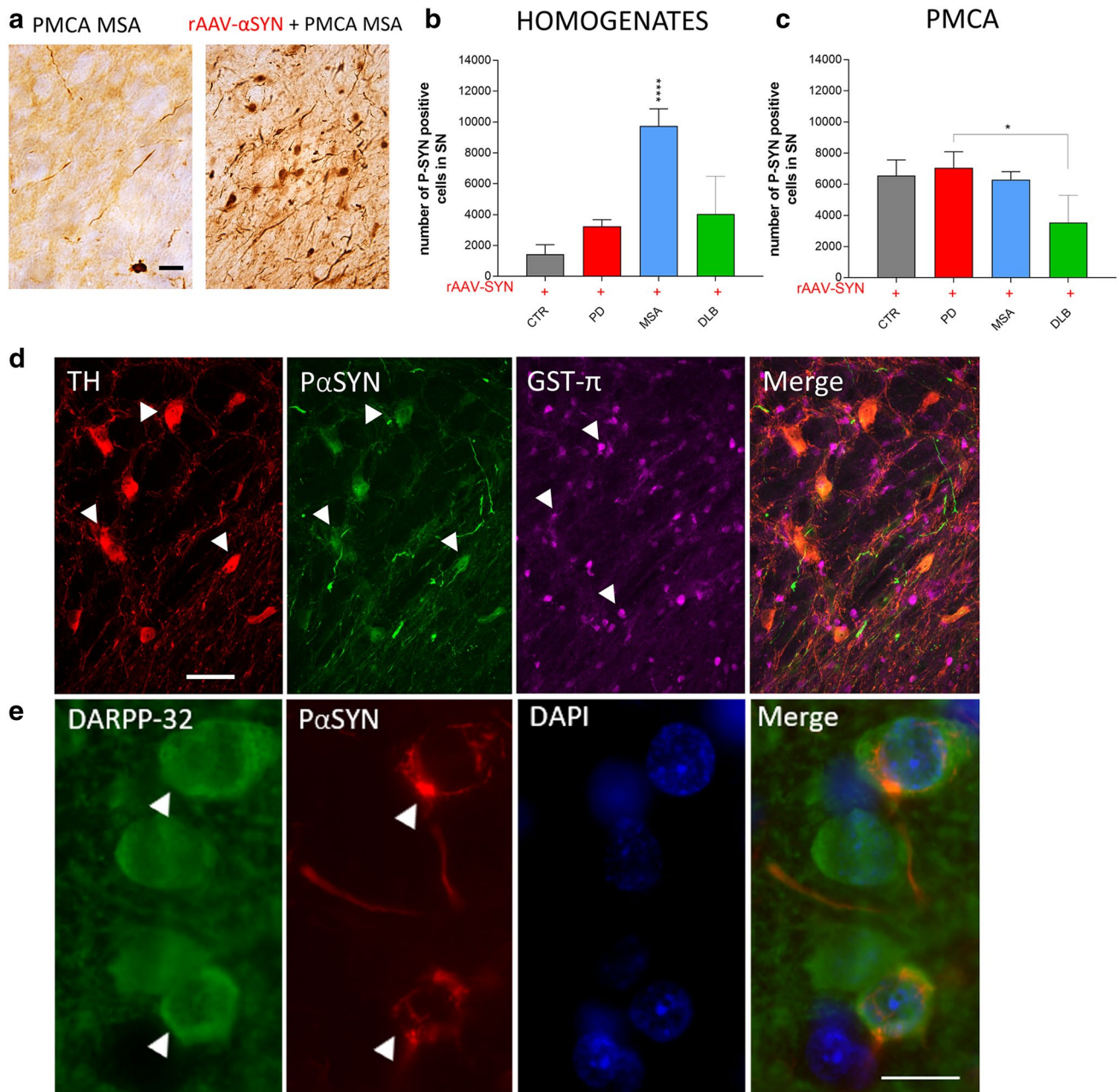


Fig. 7 Assessment of α SYN pathology after intracerebral inoculation of different patient-derived homogenates and PMCA-amplified α SYN assemblies in association with rAAV2/7-mediated α SYN expression. **a** Representative images of a P-S129 α SYN staining in the SN 5 months after co-injection of PMCA-amplified MSA strains in absence (left) or presence (right) of rAAV2/7- α SYN overexpression. Scale bar = 50 μ m. **b**, **c** Stereological quantification of the number of P α SYN⁺ cells in the SN 5 months after co-injection of patient-derived homogenates (**b**) or PMCA-amplified α SYN assemblies (**c**) with rAAV2/7- α SYN overexpression. Results shown as mean \pm SEM ($*p < 0.05$, $****p < 0.0001$ for one-way ANOVA with Tukey's post-hoc analysis, $n = 4-6$ patients per group and $n = 3$ per patient). A total of 12–16 animals per group was included in this study. **d** Representa-

tive images of dopaminergic neurons (TH, in red), α SYN phosphorylated at Ser129 (P-S129 α SYN, in green) and oligodendrocytes (GST- π , in magenta) in the SN 5 months after inoculation of PMCA-amplified MSA strains in association with rAAV2/7-mediated overexpression of α SYN. White arrowheads represent on the one hand neuronal cell bodies (red) co-localizing with P-S129 α SYN staining (green) and on the other hand oligodendroglia cell bodies (magenta) in the absence of co-localization with P-S129 α SYN (green). Scale bar represents 50 μ m. **e** Representative image of striatal medium spiny neurons (DARPP-32, in green) and α SYN phosphorylated at Ser129 (P-S129 α SYN, in red) in the striatum 5 months after inoculation of PMCA-amplified MSA strains in association with rAAV2/7-mediated overexpression of α SYN

rAAV- α SYN + HOMOGENATES

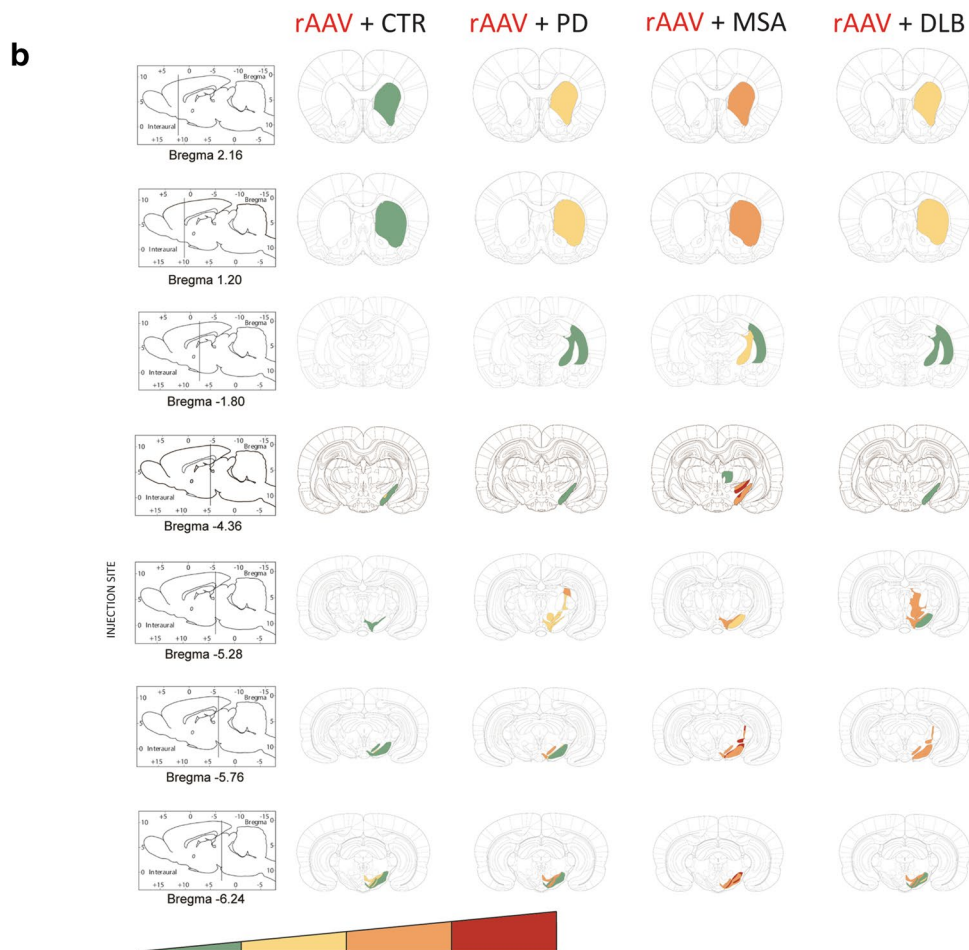
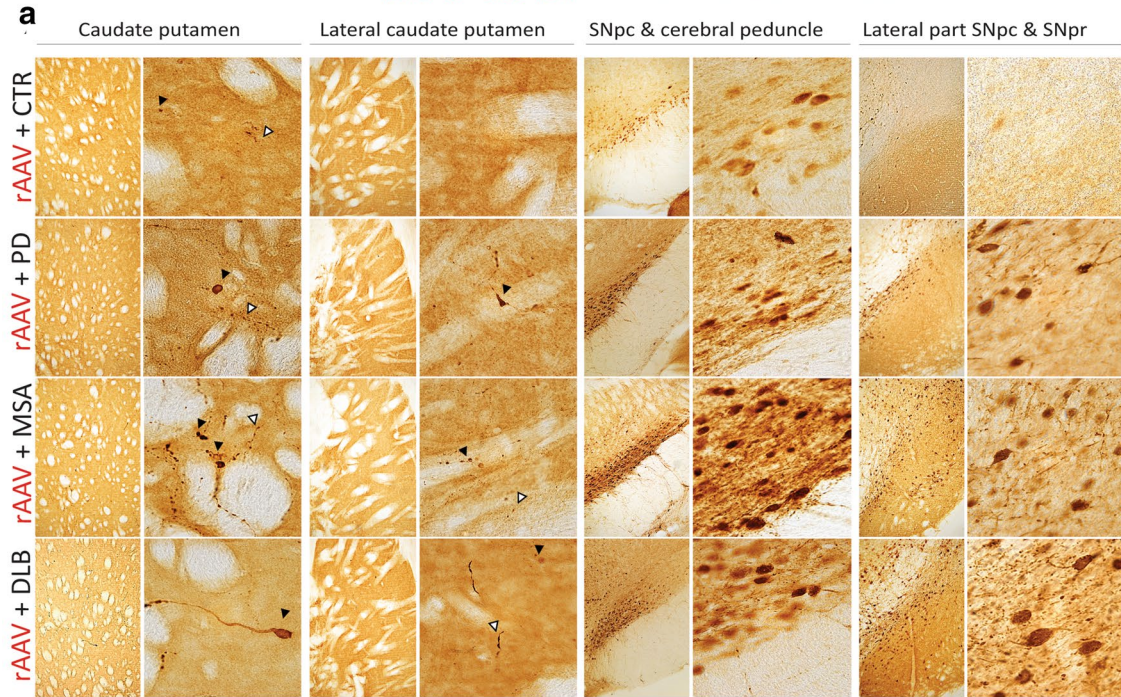


Fig. 8 Spreading of α SYN pathology after inoculation of different patient-derived homogenates. **a** Representative photomicrographs of P α SYN pathology in four different brain regions 5 months after co-injection of patient-derived homogenates and rAAV2/7- α SYN over-expression. The selected brain regions are the following: (1) and (2) adjacent sections of caudate putamen (CPu); (3) SNpc and cerebral peduncle (cp); (4) lateral part of the SNpc and SNpr. Black arrows represent P α SYN positive cells and open arrows show P α SYN-positive outgrowths. Scale bars represent 200 μ m (left) and 50 μ m (right). **b** Heat map for the spreading of α SYN pathology towards different brain regions. The heat map ranges from low (green) to very high (red). A total of three animals per group was included. The data were presented as heat maps to semi-quantitatively illustrate the distribution of α SYN pathology throughout the brain. Each panel represents a coronal plane (bregma 2.16, 1.20, -1.80, -4.36, -5.28, -5.76, -6.24 mm) for each group. The left column presents sagittal views of the corresponding coronal planes

9b). The latter results are altogether in agreement with the limited effect of DLB patient-derived PMCA assemblies on motor behavior (Fig. 5f) and nigral and striatal cell loss (Fig. 6e, j). We further examined the presence of P α SYN pathology in other cell types such as astrocytes (data not shown) and oligodendrocytes but we only found P α SYN positive neuronal inclusions in the SN (Fig. 7d) or the striatum (Fig. 7e).

Next, we assessed the distribution pattern of pathological α SYN within the brain following injection of PD, MSA and DLB patient brain homogenates and the corresponding PMCA-amplified assemblies with or without rAAV-driven α SYN expression (Figs. 8, 9). For patient brain homogenates, α SYN phosphorylation patterns in brain regions connected to the injection site were only seen upon co-injection with rAAV- α SYN (Fig. 8a, b). Pathological α SYN deposits were more abundant for all diseases compared to controls but most prominent in animals injected with MSA patient brain homogenates. Both P α SYN positive cells as well as P α SYN positive neurites were observed in the dorsal caudate putamen. A considerable number of P α SYN positive cells and very few P α SYN positive neurites were observed in the SN (Fig. 8a). Interestingly, PMCA-amplified assemblies induced an overall more pronounced P α SYN pathology compared to the patient brain homogenates. The sole injection of PMCA-amplified MSA assemblies induced the most prominent spreading of pathological α SYN deposits in the regions almost similar to those observed with combined injection of rAAV- α SYN and MSA patient brain homogenates (the caudate putamen and the lateral part of the SN, Figs. 7e, 9a, c). However, P α SYN positive neurites were more abundant than P α SYN positive cells. Furthermore, co-injection of rAAV- α SYN and PMCA-amplified MSA assemblies led to a more severe phenotype (Fig. 9b, d). Here, both P α SYN positive cells and P α SYN positive neurites were found in the different brain regions examined. Again, PMCA-amplified DLB assemblies with or without

rAAV- α SYN induced very low levels of P α SYN pathology in the striatum, similar to the CTR animals.

The overall amount of aggregated α SYN in the brains of animals who received PD, MSA and DLB patient-derived PMCA-amplified α SYN assemblies together with rAAV- α SYN vector was also quantified using the HTRF Cisbio assay [14]. The amounts of aggregated α SYN in animals injected with PMCA-amplified MSA assemblies were significantly and consistently higher than that of animals of any other group (Fig. 10).

PD, MSA, and DLB patient-derived α SYN strains trigger a differential immune response

To investigate whether distinct α SYN strains may act as antigens altering immune tolerance, provoking neuroinflammation and subsequent deleterious reactions, we investigated the presence of different immune-related cells in the brain. In naive animals, injection of different brain homogenates or PMCA-amplified α SYN strains did not induce a detectable Iba1 positive microglial response at the final time point of 150 days (data not shown). However, in the presence of human α SYN, we detected a pronounced additive immune response. Remarkably, the overall immune response to PMCA-amplified α SYN assemblies from PD, MSA and DLB patients was more significant compared to the corresponding brain homogenates. When comparing diseases, MSA-derived material induced the strongest immune response, followed by PD and DLB (Fig. 11). More specifically, co-injection of PD or MSA brain homogenates or PMCA-amplified α SYN strains with rAAV- α SYN resulted in a significantly higher number of Iba1 positive cells and the presence of large phagocytic reactive microglia (Fig. 11a, b). Major histocompatibility complex class II (MHC II) expression was triggered by injection of PD, MSA and DLB material, with the strongest expression for samples originating from MSA patients (Fig. 11a, b). Since microglial upregulation of MHC II is suggestive of an adaptive immune response, we further examined the affected areas for CD4 (helper) and CD8 (cytotoxic) T cell infiltration. An increase in the number of CD4 and CD8 positive T cells paralleled MHCII expression (Fig. 11a, b).

Discussion

The discovery that α SYN assembles into structurally distinct fibrillar assemblies has led to the hypothesis that those assemblies, also referred to as ‘strains’, could account for the different clinicopathological traits within synucleinopathies [9, 36]. In a previous study, we brought evidence for a structural-pathological relationship for α SYN strains in

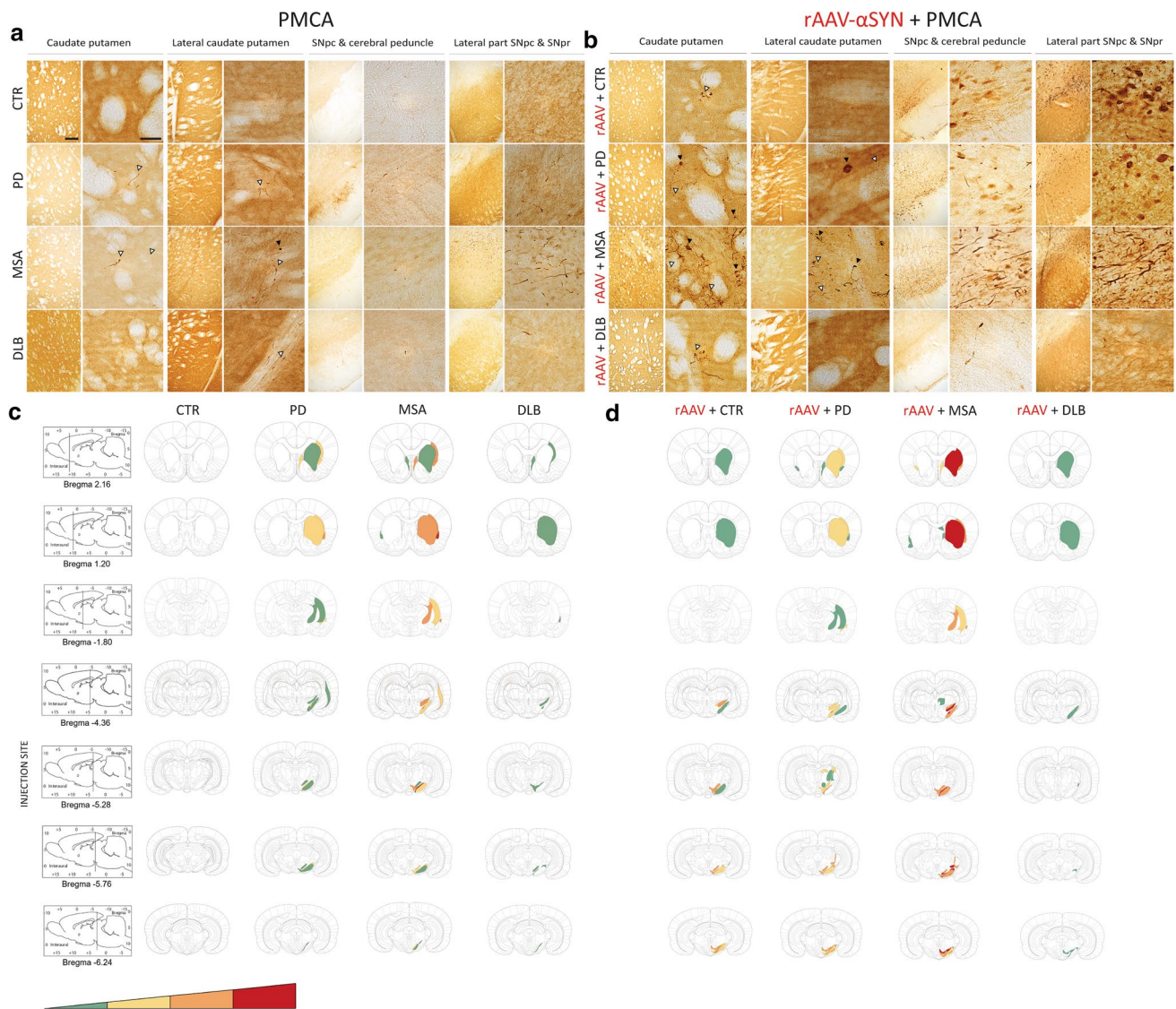


Fig. 9 Spreading of α SYN pathology after inoculation of different PMCA-amplified α SYN strains. **a, b** Representative photomicrographs of P α SYN pathology in four different brain regions 5 months after inoculation of PMCA-amplified α SYN assemblies without (**a**) or with (**b**) rAAV2/7- α SYN expression. The selected brain regions are the following: (1) and (2) adjacent sections of caudate putamen (CPu); (3) SNpc and cerebral peduncle (cp); (4) lateral part of the SNpc and SNpr. Black arrows represent P α SYN positive cells and open arrows show P α SYN-positive outgrowths. Scale bars represent 200 μ m (left) and 50 μ m (right). (**c–d**) Heat map for the spreading of

α SYN pathology towards different brain regions after inoculation of PMCA-amplified α SYN assemblies without (**c**) or with (**d**) rAAV2/7- α SYN expression. The heat map ranges from low (green) to very high (red). A total of three animals per group was included. The data were presented as heat maps to semi-quantitatively illustrate the distribution of α SYN pathology throughout the brain. Each panel represents a coronal plane (bregma 2.16, 1.20, -1.80, -4.36, -5.28, -5.76, -6.24 mm) for each group. The left column presents sagittal views of the corresponding coronal planes

synucleinopathies, by showing that two recombinant α SYN fibrillar polymorphs, which possessed different structural and seeding properties, trigger distinct histopathological and behavioral phenotypes in vivo [36]. Here, we present evidence that distinct α SYN strains exist in well-stratified cohorts of PD, MSA and DLB patients. We used the seeding propensity of aggregated α SYN in diseased human brain homogenates in an ex vivo assay inspired by the PMCA

method [17] to amplify and generate pure and homogenous assemblies of α SYN that are disease-specific. Our observations reveal unique seeding features of brain homogenates from patients who developed PD, DLB or MSA in agreement with observations made using a different amplification method [11]. Besides exhibiting different shapes upon TEM analysis, the amplified fibrillar assemblies showed distinct fingerprints, characteristic of PD, MSA and DLB. Indeed,

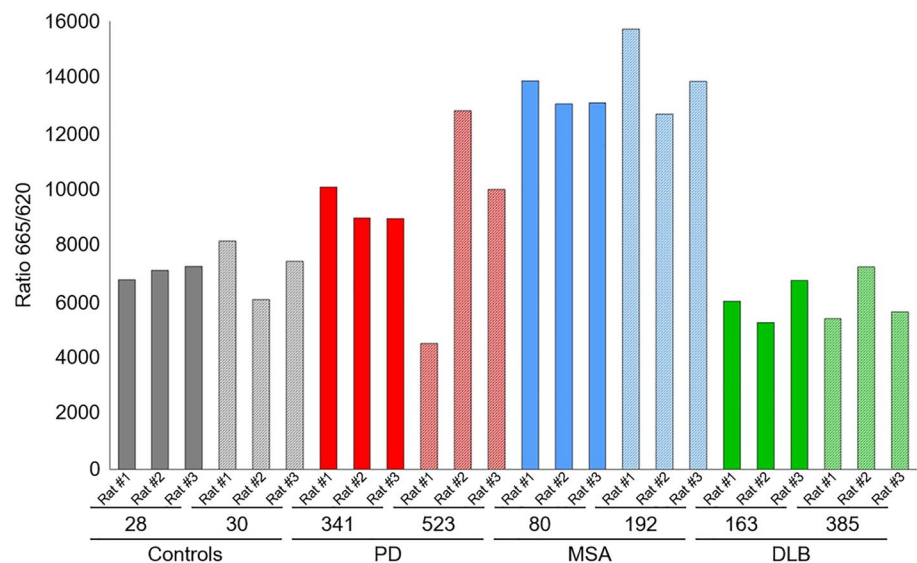
the limited proteolysis patterns of PD and MSA patient-derived fibrils shared significant similarities and differed from those derived from DLB patients. The proteolysis pattern of PD and MSA patient-derived fibrils resembled that of the fibrillar polymorph ‘Ribbons’ while the pattern of DLB patient-derived fibrils was similar to the fibrillar polymorph ‘Fibrils’. In addition, PD and MSA patient-derived fibrils are overall recognized to a lesser extent than DLB patient-derived fibrils by the aggregated α SYN-specific antibody FILA4. Altogether, these findings strongly suggest that pathogenic α SYN in PD, DLB and MSA has distinct structural traits that are characteristic of each synucleinopathy and can be reproduced through the amplification assay we implemented. Our data further indicate that TEM analysis, proteolytic and conformational antibodies profiling provide complementary information, critical to distinguish one synucleinopathy from another. Our results are in partial agreement with a recent study demonstrating similarities between PMCA-amplified fibrils derived from PD and MSA patient brains, although significant structural diversity between individual patients was also reported, while we found mostly similarities between patients from the same disease [52].

In a cellular seeding assay and in primary neurons, all patient-derived α SYN assemblies induced aggregation and phosphorylation of α SYN, which demonstrates the seeding capacity of all amplified fibrillar assemblies. This is in line with previously published data for recombinant α SYN seeds [29, 34, 58]. Somewhat surprisingly, and in contrast with previous published data [44], the brain homogenates did not result in significant inclusion formation under our experimental conditions. This is most probably due to the amount of seeds in the diluted brain homogenates. In addition, in spite of some variability between individual patients, we observed disease-specific differences in the number and

shape of the aggregates induced by PMCA-amplified strains. α SYN strains derived from DLB patients induced a higher number of inclusions with a longer shape compared to PD and MSA α SYN strains in the human H4 neuroglioma cells seeding assay. In primary neurons, DLB-derived α SYN strains induced diffuse P α SYN deposits within the soma surrounding the nucleus, while PD and MSA strains led to mainly neuritic linear or punctate P α SYN positive inclusions. These data suggest either differential seeding, take-up or clearing propensities for distinct patient-derived α SYN strains.

Next, we assessed the properties of patient-derived brain homogenates as well as PMCA-amplified α SYN strains after intracerebral inoculation in the rat SN. Overall, there were considerable similarities but also some differences for the different phenotypic read-outs between brain homogenates and fibrils obtained by PMCA. Of course, one needs to take into consideration that total brain homogenates are heterogeneous in nature and contain beside aggregated α SYN a mixture of proteins and probably inflammatory components, whereas PMCA-derived assemblies represent pure α SYN protein. In this regard, we propose that phenotypic traits induced by PMCA-derived assemblies may be attributed to strain-specific properties, while phenotypes induced by patient-derived homogenates may be explained by a combination of differences in strain and/or disease environment. When comparing to our previous findings for recombinant Fibrils and Ribbons in vivo, the MSA- and PD-derived strains partially resemble Ribbons with regard to the induction of α SYN pathology, while in terms of potency to induce motor deficits, dopaminergic neurodegeneration and neuroinflammation, they appear more similar to Fibrils [36]. This suggests that the patient-derived assemblies represent

Fig. 10 Quantification of aggregated α SYN in rodent brains. The amount of pathogenic, aggregated α SYN in brain homogenates of the rats (2.5%, W:V in PBS) inoculated with the PMCA-amplified α SYN assemblies derived from CTR, PD, MSA and DLB patients (5 μ l injected) and rAAV α SYN vector (0.5 μ l) was quantified using the Cisbio FRET assay as described in the “Materials and methods” section



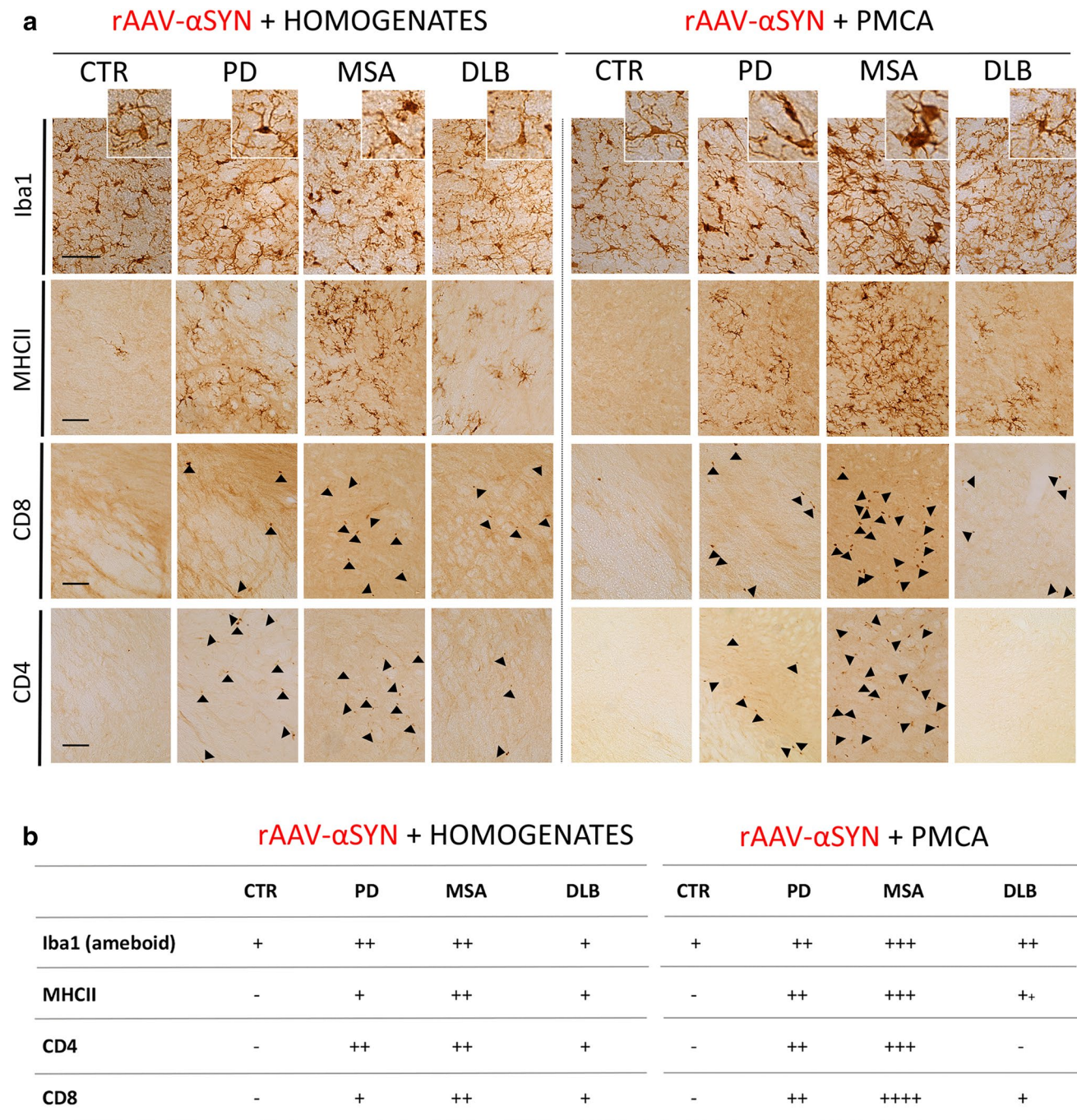


Fig. 11 Assessment of immune response after inoculation of different patient-derived homogenates and PMCA-amplified α SYN strains in association with rAAV2/7-mediated α SYN expression. **a** Representative photomicrographs of the immune response stained for Iba1 (microglia), MHCII (reactive microglia), CD4 (T helper cells) and CD8 (cytotoxic T cells) in the SN 5 months after co-injection of different patient-derived homogenates (left) or PMCA-amplified α SYN assemblies (right) with rAAV2/7- α SYN overexpression. Cells immunoreactive for CD4 and CD8 are marked with black arrows. Scale bar

Iba1 = 50 μ m, MHCII – CD4 = 100 μ m. **b** Table with scoring system for the different immune markers Iba1, MHCII, CD4 and CD8 in the rat SN 5 months after inoculation with patient-derived homogenates (left) or PMCA-amplified α SYN assemblies (right) combined with human α SYN expression. The scoring system ranges from not present (–) to abundantly present (++++). A total of three animals per group was included. The data were presented as a table with scoring system to demonstrate the presence of an inflammatory response in the rat SN

distinct strains with similarities but also differences compared to the recombinant strains.

The induction of α SYN pathology throughout the brain after inoculating MSA or DLB-derived brain homogenates in the parietal lobe, the striatum or the SN of transgenic mice has been reported previously [8, 30, 44, 63]. Progressive nigrostriatal neurodegeneration upon intranigral inoculation of PD-derived α SYN-enriched brain fractions in both mice and monkeys has also been described [45]. More recent studies using sarkosyl-insoluble α SYN fractions from brains of patients with MSA or Lewy body disease (grouping Alzheimer's disease, DLB and Parkinson's disease Dementia (PDD) together) have suggested that both the α SYN seed and its environmental context determine how α SYN strains might originate [37].

Here, to the best of our knowledge, we compared for the first time the structural and pathogenic characteristics of brain homogenates in parallel with pure PMCA-amplified α SYN strains from well-stratified synucleinopathy patients that were clinically and neuropathologically examined. MSA patient brain homogenates as well as MSA PMCA-derived strains—especially when combined with viral vector-mediated human α SYN expression—appear to be most potent in inducing motor deficits, nigrostriatal neurodegeneration, α SYN pathology and spreading, which reflects the aggressive nature of MSA. The more pronounced phenotype observed in the presence of soluble human α SYN supplied by rAAV vectors, as previously described [36, 56], is in line with the accelerated proliferation observed in transgenic M83 mice compared to wild type animals [26]. Of note, we were unable to detect clear oligodendroglial inclusions in any experimental condition, which is in agreement with previous studies [37, 44, 63]. Interestingly, PD patient-derived α SYN strain resembled the strain originating from MSA patients. The two strains had similar shapes and fingerprint. Both strains affected similarly dopaminergic neuron survival but the PD-derived α SYN strain appears to template α SYN aggregation in a less efficient manner, with as a consequence a less pronounced disease phenotype. The latter may be the consequence of either a slower growth rate, a lower resistance to clearance or to the ability of this strain to propagate from one cell to another. Our finding that DLB brain homogenates and their corresponding PMCA-amplified α SYN assemblies, appear to be much less pathogenic, yielding a milder disease phenotype was somewhat unexpected. Until now, only a limited number of studies have investigated DLB-derived α SYN strains. Amplification of the frontal cortex and the SN by RT-QuIC revealed stronger seeding activity for DLB compared to PD, but this study did not include in vivo characterization [11]. Moreover, unlike PMCA, RT-QuIC amplification reactions are performed in the presence of the dye thioflavin T. This ligand could

facilitate, through its differential binding to distinct fibrillar α SYN fibrillar assemblies [9], the formation of strains that differ from those obtained by PMCA. In addition, the brain regions examined might also be relevant, since regional variation was described for different synucleinopathies [50]. The intrinsic structure of pathogenic α SYN may depend on the local conditions of the brain region where they formed. Once formed, those aggregates propagate in a prion-like manner to other affected regions. By doing so, they imprint their intrinsic structure to endogenous monomeric α SYN. Thus, it might be interesting in the future to compare structurally seeds from different brain regions for each synucleinopathy. Finally, the differential behavior of α SYN strains was demonstrated very recently for recombinant, MSA and DLB brain-derived α SYN strains in M83 A53T- α SYN transgenic mice [26]. In agreement with our study, MSA-derived assemblies induced the most severe phenotype, while DLB assemblies did not propagate efficiently.

The recent observations that aggregated α SYN templates the aggregation of the monomeric form of the protein and spread throughout the nervous system, suggest that α SYN aggregation drives synucleinopathy progression. However, the role of inflammatory processes in this complex scenario is poorly understood. Extracellular propagation of distinct α SYN strains could alter the immune tolerance and subsequent reaction, leading to neurotoxicity through the release of pro-inflammatory cytokines. Previously, we observed brain infiltration of T cells in our rAAV2/7- α SYN rat model, suggesting a link between adaptive immunity and synucleinopathy [38]. In this study, we demonstrate a strong Iba1 and MHCII response (antigen presentation) as well as CD4 and CD8 T cell infiltration upon inoculation with PD and MSA patient-derived strains. The differential immune response toward distinct α SYN strains shows that the synucleinopathy strains represent unique antigens, which might determine disease outcome. In line with our results, well-defined α SYN peptides and structurally distinct α SYN assemblies drive helper and cytotoxic T cell responses and activate monocytes in PD patients [22, 54], thus corroborating the GWAS link to specific major histocompatibility complex alleles [2].

With this work, we characterized distinct human α SYN strains in vivo and provide new evidence that underline their relevance in synucleinopathies. We demonstrate that a specific signature can be attributed to PD, MSA and DLB-derived strains that differs from previously described recombinant strains (Table 2). Future studies investigating how distinct patient-derived α SYN strains behave when specifically targeting different brain regions (e.g. MSA strains in the basal ganglia (striatum) and the cerebellum or DLB strains in the neocortex) will further unravel this complex question. The development of highly sensitive

Table 2 The table summarizes the data obtained after inoculation with the different patient-derived homogenates (left) or PMCA-amplified α SYN assemblies (right) in association with human α SYN expression

	rAAV- α SYN + HOMOGENATES				rAAV- α SYN + PMCA			
	CTR	PD	MSA	DLB	CTR	PD	MSA	DLB
Motor deficits			+					–
DA degeneration SN		+	+			+	+	
Striatal nerve loss			+					–
α SYN pathology SN			+					–
α SYN spreading			+				++	–
Immune response			+				++	–

The following parameters are included: motor deficits, dopaminergic neuronal cell loss in the SN, striatal nerve loss, α SYN pathology in the SN, spreading of α SYN pathology and immune response. The scoring system ranges from not/mildly present (–) to strongly present (++)

rAAV α -synuclein, *DA* dopaminergic, *rAAV- α SYN* recombinant adeno-associated viral vector expressing α SYN, *SN* substantia nigra

techniques with the aim of detecting pathological α SYN strains might contribute to earlier and specific diagnosis of synucleinopathies. Therapeutic strategies specifically targeting disease-specific strains or their unique interactome might open new avenues aimed at slowing or stopping disease progression.

Acknowledgements We thank A. Aertgeerts, J. Van Asselbergs and Tracy Bellande for their technical assistance and the Leuven Viral Vector Core (LVVC) for the rAAV vector production. Confocal Images were recorded on a Zeiss LSM 880—Airyscan (Cell and Tissue Imaging Cluster (CIC), Supported by Hercules AKUL/15/37_GOH1816N and FWO G.0929.15 to Pieter Vanden Berghe, KU Leuven). We thank the KU Leuven imaging core (LiMoNe) and Nikky Corthout and Axelle Kerstens for their technical assistance. Transmission electron micrographs were obtained at the electron microscopy facility Imagerie-Gif. The FILA4 antibody was a generous gift from Poul-Henning Jensen, Danish Research Institute of Translational Neuroscience—DANDRITE, Aarhus University, Aarhus, Denmark. The present research benefited from the Electron microscopy facility of Imagerie-Gif, supported by ANR-10-INBS-04-01), and the Labex ANR-11-IDEX-0003-02. This work was supported by the FWO Flanders (Projects G.0927.14, G080517N and postdoctoral fellowship to Anke Van der Perren), the KU Leuven (OT/14/120, C14/18/102), the Flemish Parkinson Liga (VPL), Fund Sophia managed by the King Baudouin Foundation, the ERA-NET JPco-fuND 2015 SYNACTION (JPND-SYNACTION-ANR-15-JPWG-0012-03), the Medical Foundation Queen Elisabeth (PhD fellowship Géraldine Gelders), the Centre National de la Recherche Scientifique, the Fondation Simone et Cino Del Duca of the Institut de France, the Fondation Bettencourt-Schueller, the Fondation Recherche Médicale (Contract DEQ 20160334896) and the EC Joint Programme on Neurodegenerative Diseases TransPathND, ANR-17-JPCD-0002-02. This work has also received support from the European Union’s Horizon 2020 research and innovation programme and EFPIA Innovative Medicines Initiative 2 (IMPRIND grant agreement No 116060). We thank the patients and their caregivers for their participation and contributions to the study.

Author contributions AVDP coordinated, designed and conducted the cellular and in vivo experiments; GG conducted the cellular and in vivo experiments; AF analyzed the patient brain homogenates in vitro and produced the patient-derived PMCA fractions, LB overviewed the PMCA analysis and performed the TEM; FB injected the supplementary animals, WP revised the manuscript, CVH was responsible

for the rAAV production; SG provided the human brain samples and performed the clinicopathological analysis; RM designed the experiments and revised the manuscript; VB coordinated and designed the experiments and revised the manuscript. All authors approved the final manuscript.

Compliance with ethical standards

Conflict of interest The authors declare no conflict of interest.

Open Access This article is licensed under a Creative Commons Attribution 4.0 International License, which permits use, sharing, adaptation, distribution and reproduction in any medium or format, as long as you give appropriate credit to the original author(s) and the source, provide a link to the Creative Commons licence, and indicate if changes were made. The images or other third party material in this article are included in the article’s Creative Commons licence, unless indicated otherwise in a credit line to the material. If material is not included in the article’s Creative Commons licence and your intended use is not permitted by statutory regulation or exceeds the permitted use, you will need to obtain permission directly from the copyright holder. To view a copy of this licence, visit <http://creativecommons.org/licenses/by/4.0/>.

References

1. Aarsland D, Zaccai J, Brayne C (2005) A systematic review of prevalence studies of dementia in Parkinson’s disease. *Mov Disord* 20:1255–1263. <https://doi.org/10.1002/mds.20527>
2. Ahmed I, Tamouza R, Delord M, Krishnamoorthy R, Tzourio C, Mulot C et al. (2012) Association between Parkinson’s disease and the HLA-DRB1 locus. *Mov Disord* 27:1104–1110. <https://doi.org/10.1002/mds.25035>
3. Alafuzoff I, Arzberger T, Al-Sarraj S, Bodi I, Bogdanovic N, Braak H et al. (2008) Staging of neurofibrillary pathology in Alzheimer’s disease: a study of the BrainNet Europe Consortium. *Brain Pathol* 18:484–496. <https://doi.org/10.1111/j.1750-3639.2008.00147.x>
4. Alafuzoff I, Ince PG, Arzberger T, Al-Sarraj S, Bell J, Bodi I et al. (2009) Staging/typing of Lewy body related alpha-synuclein pathology: a study of the BrainNet Europe Consortium. *Acta Neuropathol* 117:635–652. <https://doi.org/10.1007/s00401-009-0523-2>

5. Baekelandt V, Claeys A, Eggermont K, Lauwers E, De Strooper B, Nuttin B et al. (2002) Characterization of lentiviral vector-mediated gene transfer in adult mouse brain. *Human Gene Therapy* 13(7):841–853. <https://doi.org/10.1089/10430340252899019>
6. Bartels T, Choi JG, Selkoe DJ (2011) α -Synuclein occurs physiologically as a helically folded tetramer that resists aggregation. *Nature* 477:107–110. <https://doi.org/10.1038/nature10324>
7. Bendor JT, Logan TP, Edwards RH (2013) The function of α -synuclein. *Neuron* 79:1044–1066. <https://doi.org/10.1016/j.neuron.2013.09.004>
8. Bernis ME, Babila JT, Breid S, Wusten KA, Wullner U, Tamguney G (2015) Prion-like propagation of human brain-derived alpha-synuclein in transgenic mice expressing human wild-type alpha-synuclein. *Acta Neuropathol Commun* 3:75. <https://doi.org/10.1186/s40478-015-0254-7>
9. Bousset L, Pieri L, Ruiz-Arlandis G, Gath J, Jensen PH, Habenstein B et al. (2013) Structural and functional characterization of two alpha-synuclein strains. *Nat Commun* 4:2575. <https://doi.org/10.1038/ncomms3575>
10. Bridi JC, Hirth F (2018) Mechanisms of α -synuclein induced synaptopathy in Parkinson's disease. *Front Neurosci* 12:80. <https://doi.org/10.3389/fnins.2018.00080>
11. Candelise N, Schmitz M, Llorens F, Villar-Pique A, Cramm M, Thom T et al. (2019) Seeding variability of different alpha synuclein strains in synucleinopathies. *Ann Neurol* 85:691–703. <https://doi.org/10.1002/ana.25446>
12. Chartier-Harlin MC, Kachergus J, Roumier C, Mouroux V, Douay X, Lincoln S et al. (2004) Alpha-synuclein locus duplication as a cause of familial Parkinson's disease. *Lancet* 364:1167–1169
13. Conway KA, Lee SJ, Rochet JC, Ding TT, Williamson RE, Lansbury PT Jr (2000) Acceleration of oligomerization, not fibrillization, is a shared property of both alpha-synuclein mutations linked to early-onset Parkinson's disease: implications for pathogenesis and therapy. *Proc Natl Acad Sci USA* 97:571–576
14. Degorce F, Card A, Soh S, Trinquet E, Knapik GP, Xie B (2009) HTRF: A technology tailored for drug discovery—a review of theoretical aspects and recent applications. *Curr Chem Genomics* 3:22–32. <https://doi.org/10.2174/1875397300903010022>
15. Desplats P, Lee HJ, Bae EJ, Patrick C, Rockenstein E, Crews L et al. (2009) Inclusion formation and neuronal cell death through neuron-to-neuron transmission of alpha-synuclein. *Proc Natl Acad Sci USA* 106:13010–13015. <https://doi.org/10.1073/pnas.0903691106>
16. Fenyi A, Coens A, Bellande T, Melki R, Bousset L (2018) Assessment of the efficacy of different procedures that remove and disassemble alpha-synuclein, tau and A-beta fibrils from laboratory material and surfaces. *Sci Rep* 8:10788. <https://doi.org/10.1038/s41598-018-28856-2>
17. Fenyi A, Leclair-Visonneau L, Clairembault T, Coron E, Neunlist M, Melki R et al. (2019) Detection of alpha-synuclein aggregates in gastrointestinal biopsies by protein misfolding cyclic amplification. *Neurobiol Dis* 129:38–43. <https://doi.org/10.1016/j.nbd.2019.05.002>
18. Gilman S, Wenning GK, Low PA, Brooks DJ, Mathias CJ, Trojanowski JQ et al. (2008) Second consensus statement on the diagnosis of multiple system atrophy. *Neurology* 71:670–676. <https://doi.org/10.1212/01.wnl.0000324625.00404.15>
19. Goedert M (2001) Alpha-synuclein and neurodegenerative diseases. *Nat Rev Neurosci* 2:492–501
20. Goedert M (2001) Parkinson's disease and other alpha-synucleinopathies. *Clin Chem Lab Med* 39:308–312. <https://doi.org/10.1515/CCLM.2001.047>
21. Griboado S, Tixador P, Bousset L, Fenyi A, Lino P, Melki R et al. (2019) Propagation of alpha-synuclein strains within human reconstructed neuronal network. *Stem Cell Reports* 12:230–244. <https://doi.org/10.1016/j.stemcr.2018.12.007>
22. Grozdanov V, Bousset L, Hoffmeister M, Bliederhaeuser C, Meier C, Madiona K et al. (2019) Increased immune activation by pathologic alpha-synuclein in Parkinson's disease. *Ann Neurol*. <https://doi.org/10.1002/ana.25557>
23. Hansen C, Angot E, Bergström AL, Steiner JA, Pieri L, Paul G et al. (2011) α -Synuclein propagates from mouse brain to grafted dopaminergic neurons and seeds aggregation in cultured human cells. *J Clin Invest* 121:715–725. <https://doi.org/10.1172/JCI43366>
24. Hobson P, Meara J (2004) Risk and incidence of dementia in a cohort of older subjects with Parkinson's disease in the United Kingdom. *Mov Disord* 19:1043–1049. <https://doi.org/10.1002/mds.20216>
25. Kordower JH, Chu Y, Hauser RA, Freeman TB, Olanow CW (2008) Lewy body-like pathology in long-term embryonic nigral transplants in Parkinson's disease. *Nat Med* 14:504–506. <https://doi.org/10.1038/nm1747>
26. Lau A, So RWL, Lau HHC, Sang JC, Ruiz-Riquelme A, Fleck SC et al. (2019) alpha-Synuclein strains target distinct brain regions and cell types. *Nat Neurosci*. <https://doi.org/10.1038/s41593-019-0541-x>
27. Li JY, Englund E, Holton JL, Soulet D, Hagell P, Lees AJ et al. (2008) Lewy bodies in grafted neurons in subjects with Parkinson's disease suggest host-to-graft disease propagation. *Nat Med* 14:501–503. <https://doi.org/10.1038/nm1746>
28. Luk KC, Kehm V, Carroll J, Zhang B, O'Brien P, Trojanowski JQ et al. (2012) Pathological α -synuclein transmission initiates Parkinson-like neurodegeneration in nontransgenic mice. *Science* 338:949–953. <https://doi.org/10.1126/science.1227157>
29. Luk KC, Song C, O'Brien P, Stieber A, Branch JR, Brunden KR et al. (2009) Exogenous alpha-synuclein fibrils seed the formation of Lewy body-like intracellular inclusions in cultured cells. *Proc Natl Acad Sci USA* 106:20051–20056. <https://doi.org/10.1073/pnas.0908005106>
30. Masuda-Suzukake M, Nonaka T, Hosokawa M, Oikawa T, Arai T, Akiyama H et al. (2013) Prion-like spreading of pathological alpha-synuclein in brain. *Brain* 136:1128–1138. <https://doi.org/10.1093/brain/awt037>
31. Masuda-Suzukake M, Nonaka T, Hosokawa M, Oikawa T, Arai T, Akiyama H et al. (2013) Prion-like spreading of pathological α -synuclein in brain. *Brain* 136:1128–1138. <https://doi.org/10.1093/brain/awt037>
32. McKeith IG, Galasko D, Kosaka K, Perry EK, Dickson DW, Hansen LA et al. (1996) Consensus guidelines for the clinical and pathologic diagnosis of dementia with Lewy bodies (DLB): report of the consortium on DLB international workshop. *Neurology* 47:1113–1124. <https://doi.org/10.1212/wnl.47.5.1113>
33. Nam MK, Han JH, Jang JY, Yun SE, Kim GY, Kang S et al. (2015) A novel link between the conformations, exposure of specific epitopes, and subcellular localization of α -synuclein. *Biochim Biophys Acta* 1850:2497–2505. <https://doi.org/10.1016/j.bbagen.2015.09.006>
34. Nonaka T, Watanabe ST, Iwatsubo T, Hasegawa M (2010) Seeded aggregation and toxicity of α -synuclein and tau: cellular models of neurodegenerative diseases. *J Biol Chem* 285:34885–34898. <https://doi.org/10.1074/jbc.M110.148460>
35. Paleologou KE, Kragh CL, Mann DM, Salem SA, Al-Shami R, Allsop D et al. (2009) Detection of elevated levels of soluble alpha-synuclein oligomers in post-mortem brain extracts from patients with dementia with Lewy bodies. *Brain* 132:1093–1101. <https://doi.org/10.1093/brain/awn349>
36. Peelaerts W, Bousset L, Van der Perren A, Moskalyuk A, Pulizzi R, Giugliano M et al. (2015) α -Synuclein strains cause distinct synucleinopathies after local and systemic administration. *Nature* 522:340–344. <https://doi.org/10.1038/nature14547>

37. Peng C, Gathagan RJ, Covell DJ, Medellin C, Stieber A, Robinson JL et al. (2018) Cellular milieu imparts distinct pathological α -synuclein strains in α -synucleinopathies. *Nature* 557:558–563. <https://doi.org/10.1038/s41586-018-0104-4>
38. Van der Perren A, Macchi F, Toelen J, Carlon M, Maris M, De Loor H et al. (2015) FK506 reduces neuroinflammation and dopaminergic neurodegeneration in an α -synuclein-based rat model for Parkinson's disease. *Neurobiol Aging* 36:1559–1568
39. Van der Perren A, Toelen J, Carlon M, Van den Haute C, Coun F et al. (2011) Efficient and stable transduction of dopaminergic neurons in rat substantia nigra by rAAV 2/1, 2/2, 2/5, 2/6.2, 2/7, 2/8 and 2/9. *Gene Ther* 18:517–527. <https://doi.org/10.1038/gt.2010.179>
40. Van der Perren A, Toelen J, Casteels C, Macchi F, Van Rompuy AS, Sarre S et al. (2015) Longitudinal follow-up and characterization of a robust rat model for Parkinson's disease based on overexpression of alpha-synuclein with adeno-associated viral vectors. *Neurobiol Aging* 36:1543–1558. <https://doi.org/10.1016/j.neurobiolaging.2014.11.015>
41. Pieri L, Madiona K, Bousset L, Melki R (2012) Fibrillar alpha-synuclein and huntingtin exon 1 assemblies are toxic to the cells. *Biophys J* 102:2894–2905. <https://doi.org/10.1016/j.bpj.2012.04.050>
42. Polymeropoulos MH, Lavedan C, Leroy E, Ide SE, Dehejia A, Dutra A et al. (1997) Mutation in the alpha-synuclein gene identified in families with Parkinson's disease. *Science* 276:2045–2047
43. Postuma RB, Berg D, Stern M, Poewe W, Olanow CW, Oertel W et al. (2015) MDS clinical diagnostic criteria for Parkinson's disease. *Mov Disord* 30:1591–1601. <https://doi.org/10.1002/mds.26424>
44. Prusiner SB, Woerman AL, Mordes DA, Watts JC, Rampersaud R, Berry DB et al. (2015) Evidence for alpha-synuclein prions causing multiple system atrophy in humans with parkinsonism. *Proc Natl Acad Sci USA* 112:E5308–5317. <https://doi.org/10.1073/pnas.1514475112>
45. Recasens A, Dehay B, Bové J, Carballo-Carbajal I, Dovero S, Pérez-Villalba A et al. (2014) Lewy body extracts from Parkinson disease brains trigger α -synuclein pathology and neurodegeneration in mice and monkeys. *Ann Neurol* 75:351–362. <https://doi.org/10.1002/ana.24066>
46. Schmitz C, Hof PR (2005) Designed-based stereology in neuroscience. *Neuroscience* 130(4):813–31. <https://doi.org/10.1016/j.neuroscience.2004.08.050>
47. Shahnawaz M, Mukherjee A, Pritzkow S, Mendez N, Rabadia P, Liu X et al. (2020) Discriminating α -synuclein strains in Parkinson's disease and multiple system atrophy. *Nature*. <https://doi.org/10.1038/s41586-020-1984-7>
48. Shrivastava AN, Bousset L, Renner M, Redeker V, Savitschenko J, Triller A et al. (2020) Differential membrane binding and seeding of distinct alpha-synuclein fibrillar polymorphs. *Biophys J* 118:1301–1320. <https://doi.org/10.1016/j.bpj.2020.01.022>
49. Shrivastava AN, Redeker V, Fritz N, Pieri L, Almeida LG, Spolidoro M et al. (2015) alpha-synuclein assemblies sequester neuronal alpha3-Na+/K+-ATPase and impair Na+ gradient. *EMBO J* 34:2408–2423. <https://doi.org/10.15252/embj.201591397>
50. Sorrentino ZA, Goodwin MS, Riffe CJ, Dhillon JS, Xia Y, Gorion KM et al. (2019) Unique alpha-synuclein pathology within the amygdala in Lewy body dementia: implications for disease initiation and progression. *Acta Neuropathol Commun* 7:142. <https://doi.org/10.1186/s40478-019-0787-2>
51. Spillantini MG, Schmidt ML, Lee VM, Trojanowski JQ, Jakes R, Goedert M (1997) Alpha-synuclein in Lewy bodies. *Nature* 388:839–840
52. Strohaker T, Jung BC, Liou SH, Fernandez CO, Riedel D, Becker S et al. (2019) Structural heterogeneity of alpha-synuclein fibrils amplified from patient brain extracts. *Nat Commun* 10:5535. <https://doi.org/10.1038/s41467-019-13564-w>
53. Sultana Z, Paleologou KE, Al-Mansoori KM, Ardah MT, Singh N, Usmani S et al. (2011) Dynamic modeling of α -synuclein aggregation in dopaminergic neuronal system indicates points of neuroprotective intervention: experimental validation with implications for Parkinson's therapy. *Neuroscience* 199:303–317. <https://doi.org/10.1016/j.neuroscience.2011.10.018>
54. Sulzer D, Alcalay RN, Garretti F, Cote L, Kanter E, Agin-Lieb J et al. (2017) T cells from patients with Parkinson's disease recognize alpha-synuclein peptides. *Nature* 546:656–661. <https://doi.org/10.1038/nature22815>
55. Sun J, Wang L, Bao H, Premi S, Das U, Chapman ER et al. (2019) Functional cooperation of alpha-synuclein and VAMP2 in synaptic vesicle recycling. *Proc Natl Acad Sci USA* 116:11113–11115. <https://doi.org/10.1073/pnas.1903049116>
56. Thakur P, Breger LS, Lundblad M, Wan OW, Mattsson B, Luk KC et al. (2017) Modeling Parkinson's disease pathology by combination of fibril seeds and alpha-synuclein overexpression in the rat brain. *Proc Natl Acad Sci USA* 114:E8284–E8293. <https://doi.org/10.1073/pnas.1710442114>
57. Theillet FX, Binolfi A, Bekei B, Martorana A, Rose HM, Stuver M et al. (2016) Structural disorder of monomeric α -synuclein persists in mammalian cells. *Nature* 530:45–50. <https://doi.org/10.1038/nature16531>
58. Volpicelli-Daley LA, Luk KC, Patel TP, Tanik SA, Riddle DM, Stieber A et al. (2011) Exogenous α -synuclein fibrils induce Lewy body pathology leading to synaptic dysfunction and neuron death. *Neuron* 72:57–71. <https://doi.org/10.1016/j.neuron.2011.08.033>
59. Wakabayashi K, Hayashi S, Kakita A, Yamada M, Toyoshima Y, Yoshimoto M et al. (1998) Accumulation of alpha-synuclein/NACP is a cytopathological feature common to Lewy body disease and multiple system atrophy. *Acta Neuropathol* 96:445–452
60. Wakabayashi K, Yoshimoto M, Tsuji S, Takahashi H (1998) Alpha-synuclein immunoreactivity in glial cytoplasmic inclusions in multiple system atrophy. *Neurosci Lett* 249:180–182
61. Wang L, Das U, Scott DA, Tang Y, McLean PJ, Roy S (2014) alpha-synuclein multimers cluster synaptic vesicles and attenuate recycling. *Curr Biol* 24:2319–2326. <https://doi.org/10.1016/j.cub.2014.08.027>
62. Wang L, Das U, Scott DA, Tang Y, McLean PJ, Roy S (2014) α -synuclein multimers cluster synaptic vesicles and attenuate recycling. *Curr Biol* 24:2319–2326. <https://doi.org/10.1016/j.cub.2014.08.027>
63. Watts JC, Giles K, Oehler A, Middleton L, Dexter DT, Gentleman SM et al. (2013) Transmission of multiple system atrophy prions to transgenic mice. *Proc Natl Acad Sci USA* 110:19555–19560. <https://doi.org/10.1073/pnas.1318268110>
64. Winner B, Jappelli R, Maji SK, Desplats PA, Boyer L, Aigner S et al. (2011) In vivo demonstration that alpha-synuclein oligomers are toxic. *Proc Natl Acad Sci USA* 108:4194–4199. <https://doi.org/10.1073/pnas.1100976108>
65. Zarranz JJ, Alegre J, Gómez-Esteban JC, Lezcano E, Ros R, Ampuero I et al. (2004) The new mutation, E46K, of alpha-synuclein causes Parkinson and Lewy body dementia. *Ann Neurol* 55:164–173. <https://doi.org/10.1002/ana.10795>

Publisher's Note Springer Nature remains neutral with regard to jurisdictional claims in published maps and institutional affiliations.